IKR Publishers

IKR Journal of Engineering and Technology (IKRJET)
Journal homepage: https://ikrpublishers.com/ikrjet/
Volume-2, Issue-3 (May-June) 2026

OPEN ACCESS
ISSN: 3107-7331 (Online)

From Ferrous Sulfate Waste to Fertilizer and Metal Powder: Thermodynamics, Process Integration, and Circular Economy Opportunities for Dual-Product Recovery

Antonio Clareti Pereira*
PhD in Chemical Engineering São Paulo University – USP Belo Horizonte – MG – Brazil

DOI:*10.5281/zenodo.20596981*

ARTICLE INFO

Article history:
Received : 25-05-2026
Accepted : 03-06-2026
Available online : 08-06-2026

Citation: Pereira, A. C. (2026). From Ferrous Sulfate Waste to Fertilizer and Metal Powder: Thermodynamics, Process Integration, and Circular Economy Opportunities for Dual-Product Recovery. *IKR Journal of Engineering and Technology (IKRJET), 2*(3), 87-116.

ABSTRACT **Original Research Article**

Ferrous sulfate is produced in large quantities by hydrometallurgical operations, steel pickling, titanium dioxide manufacturing, acid regeneration circuits, and several wastewater treatment processes. Despite numerous utilization routes, significant quantities remain underutilized or require costly disposal and stabilization. This review critically evaluates an integrated process concept for converting ferrous sulfate solutions into two commercially valuable products: ammonium sulfate fertilizer and powder-metallurgy iron. The first stage involves urea-assisted conversion of dissolved ferrous sulfate into ammonium sulfate and ferrous carbonate. Thermodynamic assessments indicate strongly favorable reaction equilibria across typical process temperatures, and the low solubility of ferrous carbonate promotes efficient iron recovery from solution. The second stage involves thermal decomposition and hydrogen reduction of ferrous carbonate to produce metallic iron powder. Available thermodynamic and kinetic studies indicate that hydrogen reduction becomes increasingly favorable at moderate temperatures and may provide a low-carbon alternative to conventional iron powder production routes. The review compares existing ferrous sulfate management strategies, discusses the chemistry of urea hydrolysis and siderite precipitation, evaluates thermodynamic and process limitations, and examines industrial opportunities associated with fertilizer and powder metallurgy markets. Particular attention is given to reaction feasibility, process integration, product quality requirements, and scale-up challenges. The analysis suggests that the proposed dual-product pathway is a promising circular economy strategy that can reduce environmental liabilities while generating two independent revenue streams from a widely available industrial residue.

Keywords: Ferrous Sulfate Valorization, Ammonium Sulfate, Siderite, Hydrogen Reduction, Powder Metallurgy Iron, Circular Economy.

Highlights

- Ferrous sulfate waste streams can be converted into ammonium sulfate fertilizer and powder metallurgy iron through an integrated valorization route.
- Thermodynamic analysis demonstrates favorable Gibbs free energy values for urea-assisted ferrous sulfate conversion and hydrogen reduction of ferrous carbonate.
- The low solubility of siderite provides a strong equilibrium-driving force for iron recovery from aqueous sulfate solutions.
- The proposed route transforms an environmental liability into two independent value streams, supporting circular economy principles

Graphical Abstract

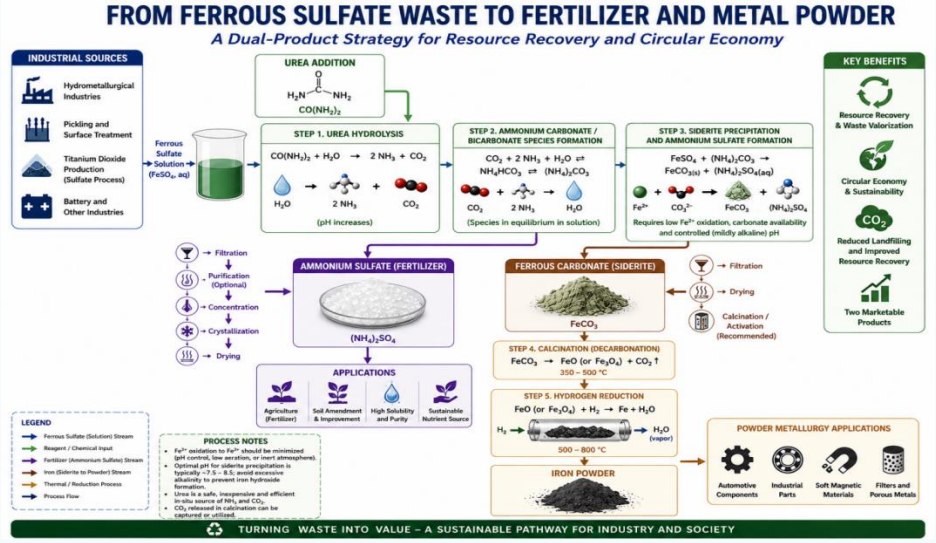

*Corresponding author: Antonio Clareti Pereira
PhD in Chemical Engineering São Paulo University – USP Belo Horizonte – MG – Brazil

Introduction

Ferrous sulfate is among the most widely generated iron-bearing residues in modern chemical, metallurgical, and hydrometallurgical industries. Significant quantities are produced during steel pickling, titanium dioxide manufacturing through the sulfate process, acid regeneration operations, hydrometallurgical circuits, mine-water treatment, and numerous industrial neutralization systems. Depending on process conditions, ferrous sulfate may be generated as crystalline $FeSO_4 \cdot 7H_2O$, partially dehydrated salts, or dissolved sulfate solutions. Although precise global production figures remain difficult to establish because many streams are internally recycled or combined with other residues before disposal, available evidence indicates that ferrous sulfate generation reaches several million tonnes annually worldwide, particularly within the steelmaking and titanium dioxide sectors (Agarwal & Pandey, 2023; Matei et al., 2022).

The growing adoption of hydrometallurgical technologies for processing low-grade ores, secondary resources, industrial residues, and recycled materials has further increased the generation of sulfate-bearing process streams. In many hydrometallurgical circuits, iron must be removed from acidic liquors to improve downstream selectivity and product quality. Depending on the process chemistry and operating conditions, this purification step frequently generates ferrous sulfate-rich solutions that require additional treatment before discharge, recycling, or final disposal (Akinwekomi et al., 2020; Cao et al., 2021). Although ferrous sulfate contains recoverable iron and sulfate values, its utilization remains limited in many regions. Traditional applications include water treatment, pigments, cement additives, soil conditioning, and feedstock for iron oxide production. However, demand for these applications often remains insufficient to absorb the quantities generated by modern industries, creating a persistent management challenge (Furmanski et al., 2024; Furmanski et al., 2025).

The disposal of ferrous sulfate streams raises both environmental and economic concerns. Sulfate-rich effluents can increase salinity in receiving waters, and residual acidity can impose additional treatment requirements. The disposal of ferrous sulfate solids has also become increasingly restricted in several jurisdictions due to concerns about long-term stability, leaching behavior, and the loss of potentially recoverable resources (Chernysh et al., 2021). Neutralization remains one of the most common treatment strategies; however, this approach typically converts dissolved iron into low-value hydroxide sludges that require subsequent handling, storage, or disposal. These practices consume reagents and eliminate opportunities for resource recovery. Similar limitations apply to stabilization and encapsulation approaches, which prioritize environmental compliance but generally fail to generate economically valuable products (Branca et al., 2020; Swain et al., 2022).

Several authors have argued that the conventional treatment paradigm treats ferrous sulfate primarily as waste rather than as a secondary resource. This perspective is increasingly at odds with current industrial priorities focused on waste minimization, resource efficiency, carbon footprint reduction, and the implementation of the circular economy. The economic burden of residue management may become substantial, particularly for large-scale hydrometallurgical operations, titanium dioxide plants, and integrated metallurgical complexes that generate continuous streams of ferrous sulfate (Vilaça et al., 2022; Wang et al., 2026).

In response to these challenges, numerous utilization routes have been investigated. Proposed approaches include producing ferric salts, synthesizing iron oxides,

manufacturing magnetic materials, preparing catalysts, recovering iron-bearing products, and using ferrous sulfate as a feedstock for environmental remediation. More recently, researchers have explored the conversion of ferrous sulfate into advanced functional materials, including adsorbents, battery-related compounds, and specialty chemical products (He et al., 2025; Du et al., 2025). Despite these advances, most valorization routes still face significant limitations. Many require multiple processing stages, high energy consumption, expensive reagents, or highly controlled operating conditions. Furthermore, several technologies yield only a single commercial product, limiting overall economic attractiveness and reducing resilience to market fluctuations. As a result, many promising technologies remain confined to laboratory-scale investigations despite encouraging technical results (Chen et al., 2025; Qiu et al., 2025).

An emerging trend in industrial sustainability research centers on integrated waste-to-value strategies that recover multiple products simultaneously from a single waste stream. These approaches aim to maximize resource efficiency and improve process economics by diversifying revenue streams. Recent studies have emphasized the importance of integrating chemical conversion, resource recovery, and circular economy principles to improve the viability of industrial residue valorization technologies (Shao et al., 2025; Wu et al., 2024). Nevertheless, relatively few investigations have explored integrated pathways that simultaneously recover both sulfate and iron values from ferrous sulfate streams. Most existing technologies prioritize either sulfate or iron recovery, rarely addressing both objectives within a unified process framework.

A further limitation of the current literature is the scarcity of studies that systematically connect reaction thermodynamics, process integration, product quality, and downstream market opportunities. Thermodynamic feasibility is frequently assumed rather than rigorously demonstrated. Consequently, several promising laboratory concepts encounter difficulties during scale-up when equilibrium constraints, impurity effects, crystallization behavior, or downstream processing requirements become important. This gap is particularly relevant for emerging circular economy technologies, where successful implementation requires simultaneous consideration of chemistry, engineering, environmental performance, and economic viability.

The combination of urea-assisted conversion of ferrous sulfate and hydrogen reduction of ferrous carbonate offers a promising alternative that directly addresses many of these limitations. In this process, sulfate is recovered as ammonium sulfate fertilizer, while iron is recovered as ferrous carbonate and then upgraded to metallic iron powder via hydrogen reduction. The resulting process generates two independent value streams from a residue that would otherwise require treatment or disposal. Furthermore, using hydrogen as a reducing agent aligns with current efforts toward low-carbon metallurgy and industrial decarbonization (Kazanc et al., 2024; Fan et al., 2025).

This review explores the scientific and technological basis of an integrated process that covers reaction thermodynamics, urea hydrolysis, ferrous carbonate precipitation, hydrogen reduction, product quality, process integration, and industrial challenges. Unlike typical reviews focusing only on ferrous sulfate, ammonium sulfate, or hydrogen metallurgy, this work examines the entire process system. Its goal is to summarize current knowledge, identify limitations and gaps, and highlight industrial opportunities in converting industrial residue into two valuable products.

Methodology

The present review was conducted using a PRISMA-informed methodology adapted for critical review studies. Unlike a systematic review focused exclusively on quantitative meta-analysis, the objective of the present work was to critically evaluate scientific, technological, thermodynamic, and industrial aspects of the integrated conversion of ferrous sulfate into ammonium sulfate and iron powder. Consequently, the literature selection process was designed to capture both fundamental studies and industrially relevant investigations.

The review covered four themes: ferrous sulfate management; urea hydrolysis and carbonate chemistry; ferrous carbonate recovery; and hydrogen-reduction pathways for iron powder. It also emphasized circular economy strategies, resource recovery, and thermodynamic modeling.

Literature searches were conducted using Scopus, Web of Science, ScienceDirect, SpringerLink, Wiley Online Library, Taylor & Francis Online, ACS Publications, MDPI, and Google Scholar. The majority of the search focused on publications from 2020 to 2026. Earlier publications were included when they provided foundational information on siderite thermodynamics, ammonium sulfate production, urea chemistry, hydrogen reduction mechanisms, or powder metallurgy.

Table 1 summarizes the search strategy adopted throughout the review.

Table 1. Search strategy, databases, and thematic coverage adopted in this review. Adapted from Page et al. (2021) and modified for the present study.

Research Topic	Main Search Terms	Primary Databases	Inclusion Focus
Ferrous sulfate generation	"ferrous sulfate waste", "iron sulfate by-product", "ferrous sulfate valorization"	Scopus, WoS, ScienceDirect	Industrial generation, waste management
Urea hydrolysis	"urea hydrolysis", "urea decomposition thermodynamics", "ammonia generation from urea"	Scopus, Springer, ACS	Reaction chemistry and thermodynamics
Siderite formation	"ferrous carbonate", "FeCO3 precipitation", "siderite thermodynamics"	Scopus, ScienceDirect	Precipitation, solubility, stability
Ammonium sulfate production	"ammonium sulfate crystallization", "fertilizer production"	Scopus, Wiley	Recovery and product quality
Hydrogen reduction	"siderite reduction", "hydrogen ironmaking", "iron powder production"	WoS, ScienceDirect	Thermodynamics and kinetics
Circular economy	"waste valorization", "resource recovery", "industrial symbiosis"	Scopus, MDPI	Sustainability assessment

Table 1 illustrates that the literature search was structured around the major stages of the proposed process chain rather than around isolated technologies. This approach facilitated identification of studies that could contribute to understanding process integration, which remains insufficiently explored in the current literature.

The screening procedure is summarized in Figure 1.

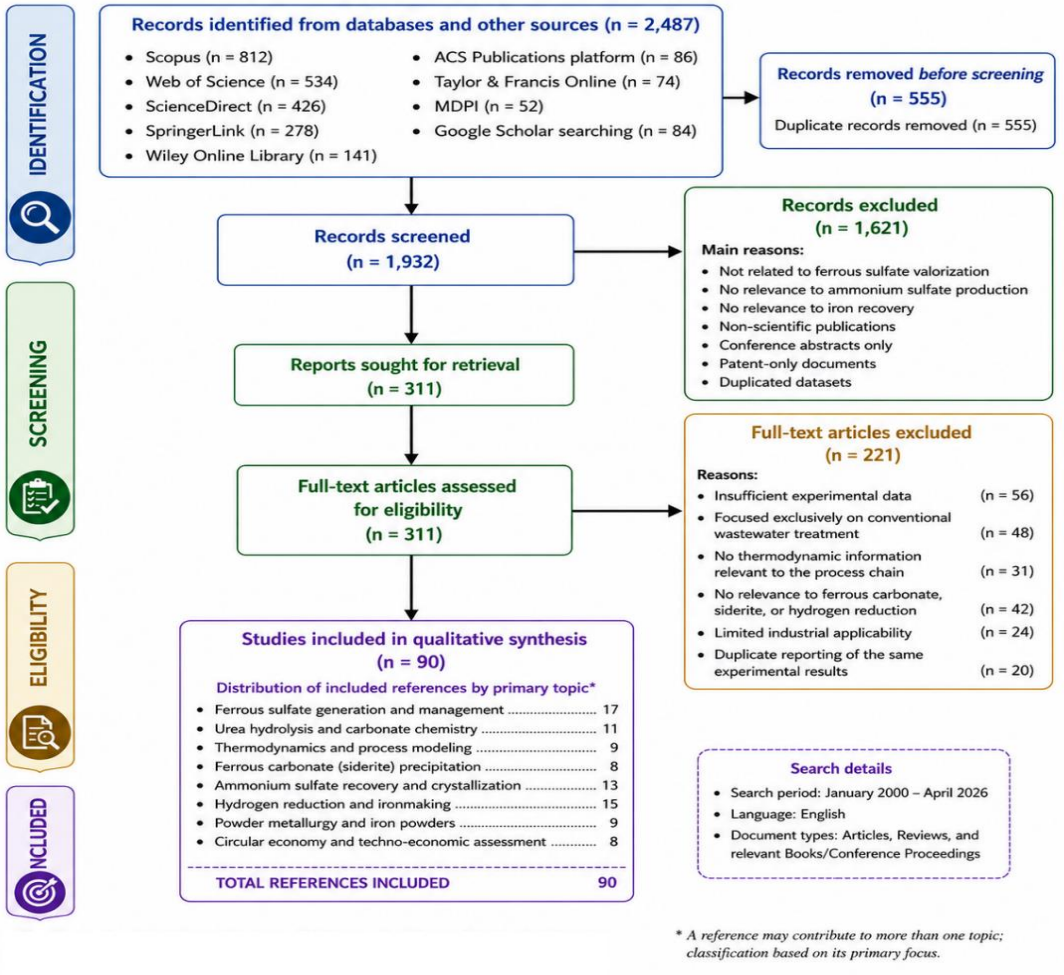

Figure 1. PRISMA-informed flowchart describing literature identification, screening, eligibility assessment, and final inclusion. Adapted from Page et al. (2021).

Figure 1 summarizes the PRISMA 2020-informed methodology adopted for literature identification, screening, eligibility assessment, and final inclusion. The initial search yielded 2,487 records from major bibliographic databases and complementary sources. Following the removal of 555 duplicate records, 1,932 unique publications were screened

based on titles and abstracts. Subsequently, 311 full-text articles were assessed for eligibility, resulting in the inclusion of 90 references in the final qualitative synthesis.

The selected literature provides the scientific basis for evaluating the integrated valorization of ferrous sulfate through urea hydrolysis, ferrous carbonate precipitation, ammonium sulfate recovery, hydrogen reduction, and iron powder production. Particular emphasis was placed on studies reporting thermodynamic data, reaction mechanisms, process performance, product quality, and industrial applicability.

To facilitate a structured critical analysis, the included references were grouped into six thematic areas: ferrous sulfate generation and management, urea hydrolysis and carbonate chemistry, ferrous carbonate precipitation, ammonium sulfate production and recovery, hydrogen reduction and ironmaking, and circular economy and techno-economic assessment. This framework supports the identification of technological advances, process limitations, and knowledge gaps discussed throughout the review.

Industrial Generation and Current Management of Ferrous Sulfate

Generation Routes

Ferrous sulfate is produced by a wide range of industrial activities that involve iron dissolution under sulfate-rich conditions. Although the chemical composition of these streams varies according to the process, the fundamental mechanism generally involves the reaction of metallic iron, iron oxides, or iron-bearing minerals with sulfuric acid. The resulting ferrous sulfate may remain dissolved in process liquors or crystallize as hydrated salts depending on temperature, concentration, and operating conditions.

Historically, the titanium dioxide industry has been one of the largest producers of ferrous sulfate. In the sulfate process, digestion of ilmenite with concentrated sulfuric acid yields substantial quantities of ferrous sulfate as a by-product. Depending on plant configuration, production rates may exceed 3–6 tonnes of ferrous sulfate heptahydrate per tonne of TiO_2 produced (Pang et al., 2020; Ibrahim et al., 2024). Although part of this material can be commercialized, market demand often remains insufficient to absorb total production.

Steel pickling operations represent another important source. Sulfuric acid pickling dissolves surface oxides and a portion of the metallic substrate, producing iron-rich sulfate solutions. While hydrochloric acid has become increasingly common in some regions, sulfuric acid pickling remains widely used due to its lower reagent cost and established infrastructure (Moreira et al., 2022a; Moreira et al., 2022b).

Hydrometallurgical processes constitute an expanding source of ferrous sulfate generation. Sulfuric acid leaching of laterites, sulfide concentrates, industrial residues, and recycled materials frequently mobilizes significant quantities of iron. Depending on redox conditions and process chemistry, iron may subsequently be removed through precipitation, solvent extraction, crystallization, or other purification steps, generating ferrous sulfate-rich streams (Xing et al., 2021).

Acid mine drainage treatment and wastewater neutralization systems also contribute to the generation of ferrous sulfate. In such cases, sulfate concentrations may vary considerably depending on mineralogy, oxidation conditions, and treatment strategy (Yuzer et al., 2022; Zhang et al., 2020).

Ferrous sulfate is produced by industries such as hydrometallurgy, steel pickling, titanium dioxide production, and chemical manufacturing. Although often a waste, it contains valuable iron and sulfate that can be recovered. Production quantities, compositions, hydration levels, impurities, and handling methods differ across industries, presenting unique recovery challenges and opportunities. Table 2 summarizes these sources and issues.

Table 2. Major industrial sources of ferrous sulfate, typical production characteristics, and management challenges. Adapted from Pang et al. (2020), Ibrahim et al. (2024), Moreira et al. (2022a), Moreira et al. (2022b), and Xing et al. (2021).

Source	Typical Ferrous Sulfate Form	Approximate Generation Rate	Main Impurities	Main Challenge
TiO_2 sulfate process	$FeSO_4 \cdot 7H_2O$	3–6 t/t TiO_2	Ti, Mn, Mg	Excess production
Steel pickling	Dissolved $FeSO_4$	30–150 g/L Fe	Acid, chlorides	Liquor treatment
Hydrometallurgy	Dissolved $FeSO_4$	Process dependent	Al, Mn, Cu, Zn	Iron removal
Acid mine drainage	Dissolved $FeSO_4$	Highly variable	Sulfates, trace metals	Environmental compliance
Wastewater treatment	Mixed sulfate streams	Variable	Multiple contaminants	Disposal cost

Table 2 shows that ferrous sulfate generation occurs across multiple industries, highlighting a recurring challenge and increasing interest in resource recovery to convert this residue into marketable products.

Existing Utilization Routes

Numerous utilization pathways have been proposed for ferrous sulfate. Traditional applications include water treatment, pigment manufacture, cement additives, and

micronutrient fertilizers. More recently, researchers have explored conversion into iron oxides, magnetic materials, catalysts, battery precursors, and advanced functional materials (Chen et al., 2025; Jiang et al., 2023).

Several studies have investigated thermal conversion of ferrous sulfate into iron oxide products. These approaches can generate materials suitable for pigments, magnetic applications, or metallurgical feedstocks. However, energy requirements may become significant because decomposition temperatures commonly exceed 500–700 °C (Ren, 2025).

Alternative approaches focus on recovering sulfate rather than iron. In these systems, sulfate is converted into fertilizer products or recovered as sulfuric acid. Although technically attractive, many of these routes leave residual iron-containing by-products that still require management (Qiu et al., 2025; Shao et al., 2025).

More recently, integrated recovery concepts have emerged. These approaches aim to maximize resource efficiency by recovering multiple components simultaneously from waste streams. Examples include combined iron-sulfate recovery systems, integrated crystallization processes, and hybrid chemical conversion routes (Furmanski et al., 2024; Furmanski et al., 2025).

The current industrial utilization landscape is summarized in Figure 2.

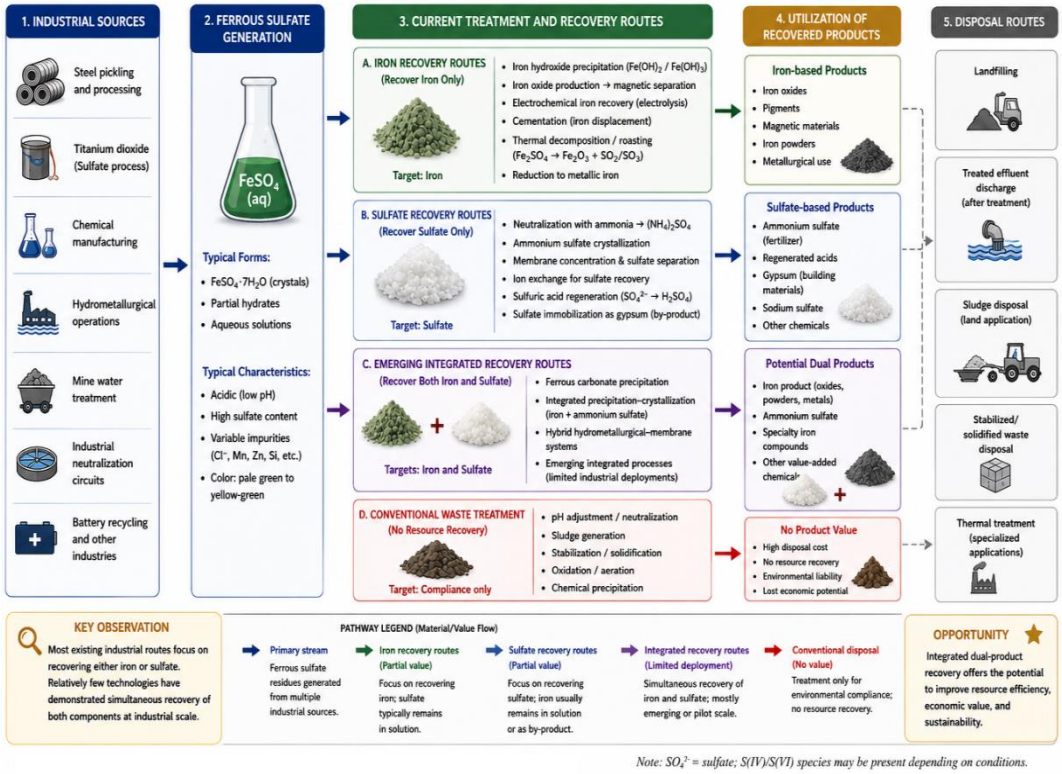

Figure 2. Current industrial pathways for the generation, treatment, utilization, and disposal of ferrous sulfate. Adapted from Chen et al. (2025), Furmanski et al. (2024), Furmanski et al. (2025), and Jiang et al. (2023).

Figure 2 illustrates that most current routes focus on either iron recovery or sulfate recovery. Few technologies effectively recover both components simultaneously, creating an important opportunity for integrated process development.

Limitations of Current Practices

Despite decades of research, several limitations continue to hinder large-scale ferrous sulfate valorization. First, many proposed technologies remain economically dependent on local market conditions. Products such as pigments or specialty iron oxides may command high value but often have limited market size.

Second, many recovery routes require significant energy input. Thermal decomposition, roasting, calcination, and advanced purification steps may substantially increase operating costs. Consequently, favorable laboratory results do not always translate into industrial viability (Branca et al., 2020).

Third, some technologies simply transfer the environmental burden from one waste stream to another. Sulfate recovery routes may generate iron-rich residues, while iron recovery routes may generate sulfate-rich liquors requiring further treatment. Such approaches improve only part of the problem (Swain et al., 2022).

A further challenge concerns process integration. Most existing studies evaluate isolated unit operations rather than complete process chains. As a result, interactions among reaction thermodynamics, crystallization behavior, product quality, energy consumption, and market value remain insufficiently understood (Vilaça et al., 2022).

These limitations help explain why large quantities of ferrous sulfate continue to be treated as residues despite containing potentially valuable iron and sulfate resources. They also motivate the development of integrated approaches capable of simultaneously recovering both components. Among the proposed alternatives, urea-assisted conversion into ammonium sulfate and ferrous carbonate is particularly interesting because it directly addresses the dual recovery challenge while relying on relatively simple chemistry and favorable thermodynamics.

The next section examines the chemical and thermodynamic foundations of urea hydrolysis and carbonate generation, which constitute the first stage of the proposed dual-product recovery pathway.

Urea Hydrolysis and Carbonate Chemistry

Urea Hydrolysis

Urea is one of the most widely produced nitrogen-containing chemicals worldwide. Annual production exceeds 180 million tonnes, largely driven by fertilizer applications. Its availability, low cost, high nitrogen content (46 wt.%), and ease of transportation make it an attractive reagent for industrial chemical conversion processes. In contrast to ammonia, urea can be stored and transported without pressurized systems, reducing logistical complexity and safety concerns (Yahya et al., 2021).

The hydrolysis of urea has been extensively studied in environmental engineering, agriculture, wastewater treatment, and mineral carbonation. The reaction may occur thermally or catalytically, producing ammonia and carbon dioxide according to:

$$CO(NH_2)_2 + H_2O \rightarrow 2NH_3 + CO_2$$

The generated ammonia subsequently reacts with water to form ammonium and hydroxyl ions:

$$NH_3 + H_2O \rightleftharpoons NH_4^+ + OH^-$$

Simultaneously, carbon dioxide dissolves and participates in a series of acid-base equilibria that ultimately generate bicarbonate and carbonate ions. These species are essential for siderite precipitation and therefore play a central role in the process evaluated in this review (Krum et al., 2021; Kuntz et al., 2021).

Several studies have reported that hydrolysis rates increase substantially above 60–70 °C. Below this range, reaction kinetics may become relatively slow, although equilibrium considerations remain favorable at longer residence times. Consequently, temperature selection represents one of the key operational variables affecting overall process performance.

Thermodynamic Aspects of Urea Decomposition

While kinetic limitations are important, thermodynamic feasibility determines whether urea hydrolysis can provide sufficient ammonia and carbonate species for subsequent conversion reactions. The HSC Chemistry simulations discussed in this review indicate that Gibbs free energy decreases steadily as temperature increases.

Table 3 summarizes the thermodynamic parameters calculated for urea hydrolysis.

Table 3. Thermodynamic parameters for urea hydrolysis calculated using HSC Chemistry. Adapted from Harvey et al. (2020), Jung and Van Ende (2020), and HSC Chemistry simulations performed for the present review.

Temperature (°C)	ΔH (kcal/mol)	ΔS (cal/mol·K)	ΔG (kcal/mol)	K	Log K
0	30.246	90.941	5.405	4.73×10^{-5}	-4.325
10	28.765	85.522	4.549	3.08×10^{-4}	-3.512
20	28.666	85.181	3.695	1.76×10^{-3}	-2.755
30	28.538	84.750	2.846	8.88×10^{-3}	-2.052
40	28.391	84.273	2.001	4.01×10^{-2}	-1.396
50	28.232	83.774	1.160	1.64×10^{-1}	-0.785
60	28.066	83.267	0.325	6.12×10^{-1}	-0.213
70	27.895	82.761	-0.505	2.10	0.322
80	27.721	82.261	-1.330	6.66	0.823
90	27.545	81.771	-2.150	19.68	1.294
100	27.369	81.292	-2.965	54.58	1.737

Table 3 shows a clear thermodynamic transition occurring near 65–70 °C. Below this range, positive Gibbs free energy values indicate that hydrolysis is not favored under standard conditions. However, the strong positive entropy contribution causes ΔG to decrease continuously with temperature. Above approximately 70 °C, the reaction becomes spontaneous, and the equilibrium constant exceeds unity.

This behavior has important process implications. First, it indicates that moderate temperatures are sufficient to activate the chemical pathway without requiring excessive energy input. Second, it suggests that waste heat available in many hydrometallurgical operations may be sufficient to support urea decomposition. Third, it demonstrates that urea can act simultaneously as a nitrogen source and an in situ carbonate

precursor, eliminating the need for external ammonia and carbonate reagents.

The thermodynamic transition identified in Table 3 will be particularly important in Section 5, where urea hydrolysis is coupled with the conversion of ferrous sulfate.

Carbonate Equilibria and Speciation

The carbon dioxide generated during urea hydrolysis undergoes a series of equilibrium reactions in aqueous solution. The distribution among dissolved CO_2, carbonic acid, bicarbonate, and carbonate depends strongly on pH, temperature, ionic strength, and dissolved metal concentrations.

The principal equilibria are:

$CO_2 + H_2O \rightleftharpoons H_2CO_3$

$H_2CO_3 \rightleftharpoons HCO_3^- + H^+$

$HCO_3^- \rightleftharpoons CO_3^{2-} + H^+$

At acidic pH values, dissolved CO_2 and bicarbonate dominate. Between pH 6 and 10, bicarbonate becomes the predominant species. At higher pH values, carbonate concentrations increase substantially, promoting precipitation of sparingly soluble carbonates such as $FeCO_3$ (Czaplicka & Konopacka-Łyskawa, 2020).

Several investigations have demonstrated that carbonate speciation controls precipitation efficiency more strongly than total dissolved inorganic carbon concentration. Consequently, process performance depends not only on urea dosage but also on pH control and reaction environment (Koo & Kim, 2020; Jiang & Tosca, 2020).

A recurring contradiction in the literature concerns the role of carbon dioxide excess. Some studies report improved carbonate formation with increasing CO_2 availability, whereas others observe partial redissolution of precipitated siderite. These apparently conflicting observations can be reconciled through speciation analysis. Excess CO_2 shifts equilibria toward bicarbonate formation, which may increase iron solubility under certain conditions (Mulders et al., 2021; Neerup et al., 2023).

Implications for Siderite Formation

Siderite precipitation represents the critical link between urea hydrolysis and iron recovery. Once sufficient carbonate becomes available, dissolved ferrous ions may react according to:

$Fe^{2+} + CO_3^{2-} \rightarrow FeCO_3(s)$

The low solubility of siderite provides a strong thermodynamic driving force for precipitation. Reported Ksp values typically range between 10^{-10} and 10^{-11}, although variations occur depending on temperature and solution composition (Grengs et al., 2024).

An important advantage of this mechanism is that precipitation removes iron directly from solution. According to Le Châtelier's principle, the continuous removal of Fe^{2+} via solid formation shifts the equilibrium toward further reaction, increasing overall conversion efficiency. Consequently, siderite formation is not merely a product recovery step but an active contributor to process thermodynamics.

The simultaneous recovery of sulfate and iron from ferrous sulfate solutions relies on a series of interconnected aqueous-phase reactions involving urea hydrolysis, ammonia generation, carbonate speciation, and siderite precipitation. Urea plays a dual chemical role by supplying nitrogen species that promote ammonium sulfate formation and carbon-containing species that enable ferrous carbonate precipitation. The distribution of ammonia, ammonium, bicarbonate, and carbonate species is strongly influenced by pH, temperature, ionic strength, and carbon dioxide availability, which collectively control both sulfate recovery and iron precipitation. Figure 2 summarizes the principal reaction pathways linking urea hydrolysis to ammonium sulfate production and siderite formation, highlighting the key equilibria, competing reactions, and process variables governing this integrated dual-product recovery strategy.

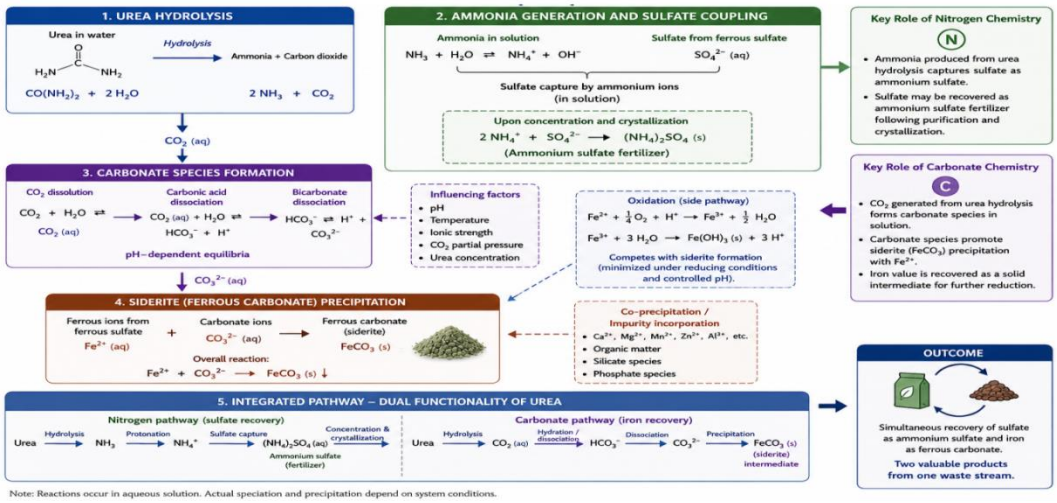

Figure 2. Reaction pathways linking urea hydrolysis, ammonia generation, carbonate speciation, and siderite precipitation. Adapted from Czaplicka and Konopacka-Łyskawa (2020), Koo and Kim (2020), Jiang and Tosca (2020), and Mulders et al. (2021).

Figure 3 illustrates how nitrogen and carbonate chemistry become coupled during the process. The generation of ammonia ultimately supports the formation of ammonium sulfate, while carbonate generation drives iron recovery through siderite precipitation. This dual functionality is one of the key features that distinguishes the proposed route from conventional ferrous sulfate treatment technologies.

The next section examines the complete thermodynamic framework governing the conversion of ferrous sulfate into ammonium sulfate and ferrous carbonate. Particular attention is given to the HSC calculations developed for this review, which provide quantitative evidence supporting the feasibility of the integrated process route.

Thermodynamic Basis of Ferrous Sulfate Conversion

The conversion of ferrous sulfate into ammonium sulfate and ferrous carbonate is the thermodynamic core of the proposed process. Unlike treatments that focus only on neutralization, this route aims to recover both sulfate and iron simultaneously. Its viability depends on whether the reaction is thermodynamically favorable in practical conditions.

Several studies highlight the importance of thermodynamic analysis in evaluating waste valorization. Laboratory success may not guarantee industrial feasibility when equilibrium constraints are significant. Quantitative assessments of Gibbs free energy, equilibrium constants, and precipitation are essential for determining whether the conversion route can achieve high recoveries efficiently (Harvey et al., 2020; Pickles & Marzoughi, 2023).

Global Reaction Pathway

The overall process can be represented by the following global reaction:

$CH_4N_2O(aq) + 2H_2O + FeSO_4(aq) \rightarrow (NH_4)_2SO_4(aq) + FeCO_3(s)$

This formulation integrates major chemical transformations. Urea provides nitrogen for ammonium sulfate and carbonate for siderite precipitation, enabling one reagent to assist in both sulfate and iron recovery.

From a process view, this dual function is a major advantage of the route. Conventional ammonium sulfate production requires ammonia, whereas siderite precipitation requires external carbonate reagents. The proposed pathway merges these into one reaction framework.

HSC Thermodynamic Assessment

The thermodynamic feasibility of the global conversion route was evaluated using HSC Chemistry. The calculations reveal that the reaction remains strongly favorable throughout the temperature range investigated.

Table 4 summarizes the thermodynamic data obtained from the simulations.

Table 4. Thermodynamic parameters calculated using HSC Chemistry for the direct conversion of ferrous sulfate into ammonium sulfate and ferrous carbonate. Adapted from Harvey et al. (2020), Jung and Van Ende (2020), and HSC Chemistry simulations performed for the present review.

T (°C)	ΔH (kcal/mol)	ΔS (cal/mol·K)	ΔG (kcal/mol)	K	Log K
0	-1.842	49.809	-15.447	2.29×10^{12}	12.361
10	-5.237	37.414	-15.831	1.66×10^{12}	12.220
20	-5.822	35.384	-16.195	1.19×10^{12}	12.075
30	-6.446	33.292	-16.539	8.40×10^{11}	11.924
40	-7.097	31.179	-16.861	5.87×10^{11}	11.768
50	-7.768	29.070	-17.162	4.05×10^{11}	11.608
60	-8.455	26.976	-17.442	2.78×10^{11}	11.443
70	-9.156	24.904	-17.702	1.88×10^{11}	11.275
80	-9.868	22.860	-17.941	1.27×10^{11}	11.104
90	-10.589	20.844	-18.159	8.50×10^{10}	10.929
100	-11.321	18.858	-18.357	5.66×10^{10}	10.753

Table 4 shows that Gibbs free energy remains negative over the 0–100 °C interval. Values vary from approximately −15.4 to −18.4 kcal/mol, indicating a strong thermodynamic driving force toward product formation.

Equally important is the magnitude of the equilibrium constants. Even at 100 °C, K remains on the order of 10^{10}. At lower temperatures, equilibrium constants exceed 10^{12}. Such values indicate that the reaction overwhelmingly favors formation of ammonium sulfate and ferrous carbonate.

A notable aspect is achieving strong thermodynamic favorability without high temperatures, setting it apart from many residue treatment methods that rely on high-temperature processes.

Thermodynamic feasibility is vital for evaluating the conversion of ferrous sulfate into ammonium sulfate and ferrous carbonate. The process involves hydrolysis, carbonate formation, sulfate capture, and precipitation, all of which are temperature-dependent. The standard Gibbs free energy

(ΔG°) and the equilibrium constant (K) indicate the spontaneity of the reaction and the stability of the products. Figure 3 shows how ΔG° and K vary with temperature, highlighting the thermodynamic driving force and the impact of temperature on equilibrium.

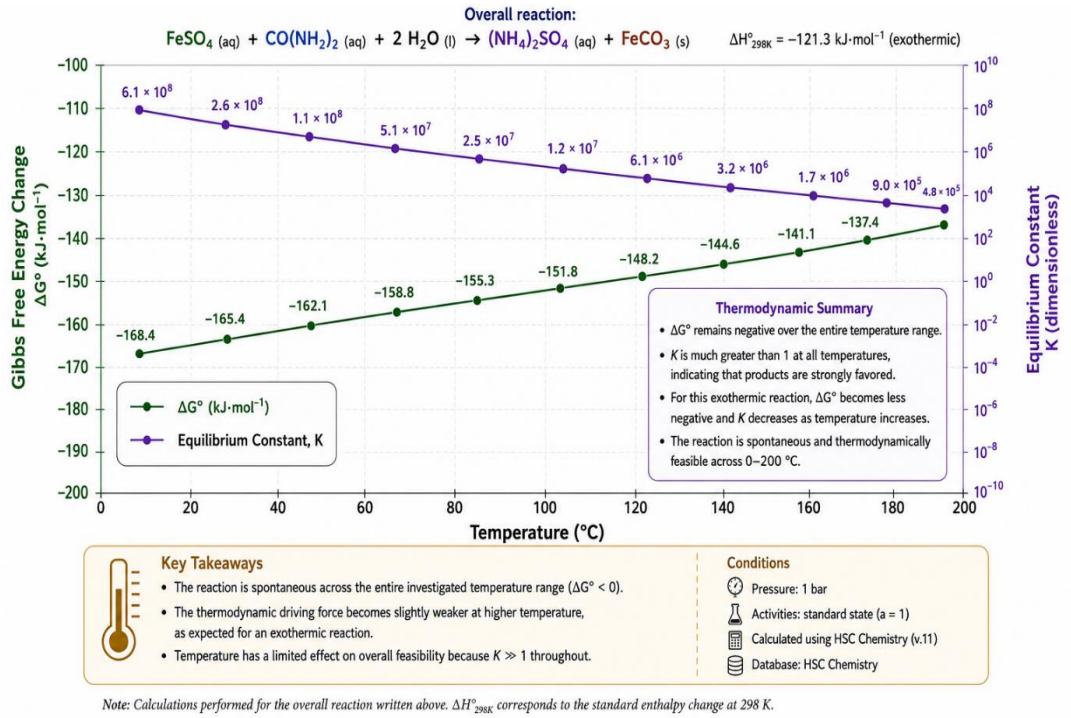

Figure 3. Temperature dependence of Gibbs free energy and equilibrium constant for the conversion of ferrous sulfate into ammonium sulfate and ferrous carbonate. Adapted from HSC Chemistry simulations performed for the present review.

Figure 4 shows that reaction spontaneity remains stable across the temperature range. The minor decrease in the equilibrium constant with increasing temperature aligns with the exothermic nature. Still, the thermodynamic driving force remains very strong throughout.

$FeCO_3$ Solubility and Precipitation

The exceptionally favorable thermodynamic behavior observed in Table 4 cannot be explained solely by the intrinsic chemistry of urea hydrolysis and ammonium sulfate formation. The precipitation of siderite plays a decisive role.

Ferrous carbonate exhibits low solubility in aqueous systems. Reported Ksp values typically fall between 10^{-10} and 10^{-11}, corresponding to pKsp values near 10.5. Such low solubility promotes efficient removal of dissolved iron.

Table 5 summarizes key parameters controlling siderite stability.

Table 5. Solubility, stability, and precipitation characteristics of ferrous carbonate in aqueous systems. Adapted from Koo and Kim (2020), Jiang and Tosca (2020), Mulders et al. (2021), Neerup et al. (2023), and Grengs et al. (2024).

Parameter	Typical Range	Process Implication
pKsp	10.3–10.8	Strong precipitation tendency
Solubility at 25 °C	<1 mg/L	Efficient iron removal
Preferred pH range	7–9	Maximized siderite formation
Excess CO_2 effect	Variable	Can increase bicarbonate formation
Fe^{2+} oxidation sensitivity	High	Requires redox control
Typical crystal size	5–200 µm	Influences filtration performance

Table 5 shows that siderite possesses favorable precipitation characteristics for industrial recovery. Once carbonate becomes available, dissolved iron can be rapidly transferred into a solid phase that can subsequently be separated through conventional solid–liquid separation operations.

Precipitation behavior isn't always straightforward; high CO_2 levels can increase bicarbonate and redissolve siderite, helping explain contradictions in optimal carbonate dosage.

Comparison with Ammonium Sulfate Production Routes

Ammonium sulfate is traditionally produced by neutralizing sulfuric acid with ammonia. Alternative routes include recovery from caprolactam production, coke-oven gas treatment, membrane-based separation systems, and sulfate conversion processes.

Typical commercial ammonium sulfate production achieves product purities above 99 wt.% and nitrogen contents of approximately 21 wt.%. Global production exceeds 20 million tonnes per year, with fertilizer applications accounting for the majority of demand (Abeyratne et al., 2023; Avşar & Ertunç, 2025).

Various technologies have been explored for sulfate recovery from industrial waste and acidic liquors, differing in source, reagents, complexity, products, and efficiency. Conventional methods mainly rely on neutralization or crystallization, while newer approaches recover sulfate with other waste components. Table 6 compares key strategies, highlighting their advantages and limitations.

Table 6. Comparison of selected sulfate recovery routes and their main characteristics. Adapted from Pang et al. (2020), Ibrahim et al. (2024), Moreira et al. (2022a), Moreira et al. (2022b), Xing et al. (2021), and the present analysis.

Route	Sulfate Source	Nitrogen Source	Main Advantage	Main Limitation
Conventional neutralization	Sulfuric acid	NH_3	Mature technology	No iron recovery
Caprolactam by-product	Process liquor	Process NH_3	Established infrastructure	Feedstock dependent
Membrane recovery	Waste streams	Variable	Sulfate recovery	Capital intensive
Proposed route	$FeSO_4$ solution	Urea	Simultaneous Fe recovery	Requires siderite management

Most technologies recover sulfate but discard or immobilize iron. Ammonia neutralization is mature but doesn't recover iron. The new method recovers sulfate as ammonium sulfate and precipitates ferrous carbonate, enabling iron reuse. This boosts resource use and reduces waste, but requires further work to improve siderite precipitation and impurity control.

Thermodynamic Feasibility of the Integrated Route

Combining thermodynamic results for urea hydrolysis and ferrous sulfate conversion shows the entire process is thermodynamically favorable at each major step. Unlike many waste valorization routes that rely on a single favorable reaction to offset downstream challenges, this sequence is supported by favorable equilibria at each stage.

The conversion of ferrous sulfate to ammonium sulfate and ferrous carbonate involves coupled equilibria like urea hydrolysis, carbonate speciation, and iron precipitation. pH controls inorganic carbon species and carbonate availability for siderite formation. Ferrous carbonate precipitation also removes Fe^{2+}, shifting equilibrium and encouraging more product formation.

Understanding interactions among carbonate chemistry, siderite precipitation, and equilibrium displacement helps identify ideal conditions and maximize recovery. Figure 5 illustrates how pH influences carbonate speciation, siderite formation, and the role of $FeCO_3$ removal in producing ammonium sulfate and ferrous carbonate.

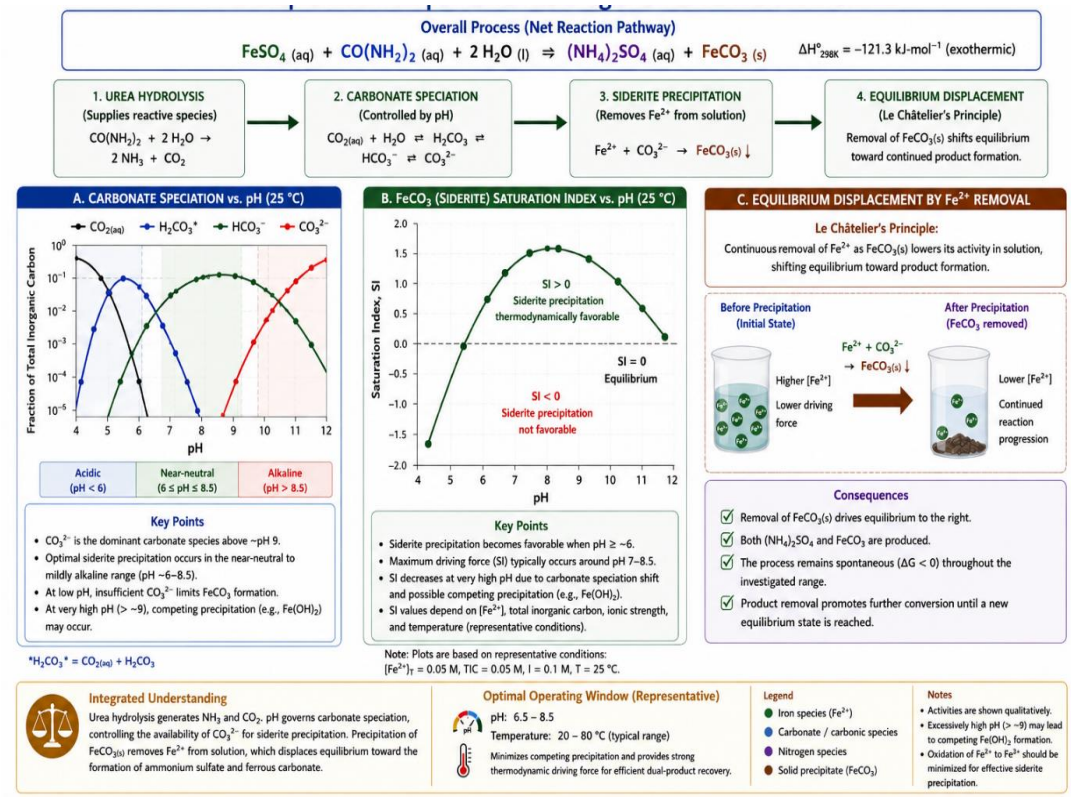

Figure 4. Influence of pH, carbonate speciation, and siderite precipitation on equilibrium displacement during ferrous sulfate conversion. Adapted from Jiang and Tosca (2020), Mulders et al. (2021), and Neerup et al. (2023).

Figure 5 summarizes the thermodynamic interactions governing the process. Urea hydrolysis supplies reactive species, carbonate speciation controls precipitation efficiency, and siderite formation removes iron from solution, continuously shifting equilibrium toward product formation.

The thermodynamic evidence supports the next steps, but successful industrial application also depends on crystal growth, filtration, purity, and handling, discussed in the next section on ferrous carbonate formation and recovery.

Ferrous Carbonate Formation and Recovery

Thermodynamic analyses show ferrous carbonate precipitation is favored under suitable conditions. Yet, industrial success also requires producing a recoverable solid with proper particle size, filtration, purity, and processability. Thus, precipitation behavior is a key stage in the dual-product recovery process.

Several studies show that carbonate precipitation's highly sensitive to supersaturation, mixing, pH, temperature, impurities, and gas-liquid transfer. Small changes can impact crystal shape and filtration. Success depends on controlling both chemistry and particle engineering.

Nucleation and Crystal Growth

Ferrous carbonate forms via nucleation and growth. Fe^{2+} reacts with carbonate from urea hydrolysis. Nucleation starts when ionic activity exceeds solubility. Low supersaturation favors crystal growth into larger particles, whereas high supersaturation promotes rapid nucleation of fine particles, increasing the risk of filtration problems and product loss (Jiang & Tosca, 2020; Mulders et al., 2021).

Temperature influences crystal growth: moderate temperatures improve diffusion and crystal development, whereas rapid precipitation leads to poorly formed particles. Siderite sizes range from a few to hundreds of micrometers, depending on conditions (Neerup et al., 2023).

Table 7 summarizes the principal parameters affecting ferrous carbonate precipitation.

Table 7. Principal operating parameters influencing ferrous carbonate precipitation, crystal growth, and solid-liquid separation. Adapted from Jiang and Tosca (2020), Mulders et al. (2021), Neerup et al. (2023), and Grengs et al. (2024).

Parameter	Typical Range	Influence on Product
Temperature	25–90 °C	Affects nucleation and growth rates
pH	7.0–9.0	Controls carbonate availability
Fe^{2+} concentration	1–100 g/L	Determines supersaturation
Carbonate concentration	Process dependent	Controls precipitation rate
Residence time	15–240 min	Influences crystal maturation
Mixing intensity	50–500 rpm equivalent	Affects particle size distribution
Typical crystal size	5–200 µm	Influences filtration performance
Solids concentration	1–20 wt.%	Influences separation efficiency

Table 7 highlights that precipitation performance depends on a combination of chemical and hydrodynamic variables. The most favorable conditions generally involve moderate supersaturation, controlled mixing, and sufficient residence time for crystal growth.

Morphology and Product Quality

Siderite morphology affects processing. Larger, denser particles settle faster, retain less moisture, and filter better. While rhombohedral crystals are typical of well-developed siderite, impurities such as magnesium, manganese, calcium, aluminum, and silica can cause irregular shapes and alter crystal habit (Grengs et al., 2024).

Impurities are vital in hydrometallurgy, as industrial solutions often contain metals that compete for carbonate ions or form precipitates, thereby impacting siderite purity and final iron powder quality.

A recurring challenge is the oxidation of Fe^{2+} to Fe^{3+}. Small amounts of oxygen ingress promote the formation of ferric hydroxides or oxyhydroxides, lowering siderite yield and contaminating the product. Industrial reactors may require inert gas blanketing or careful oxidation-reduction control.

The influence of operating variables on crystal morphology is summarized in Figure 6

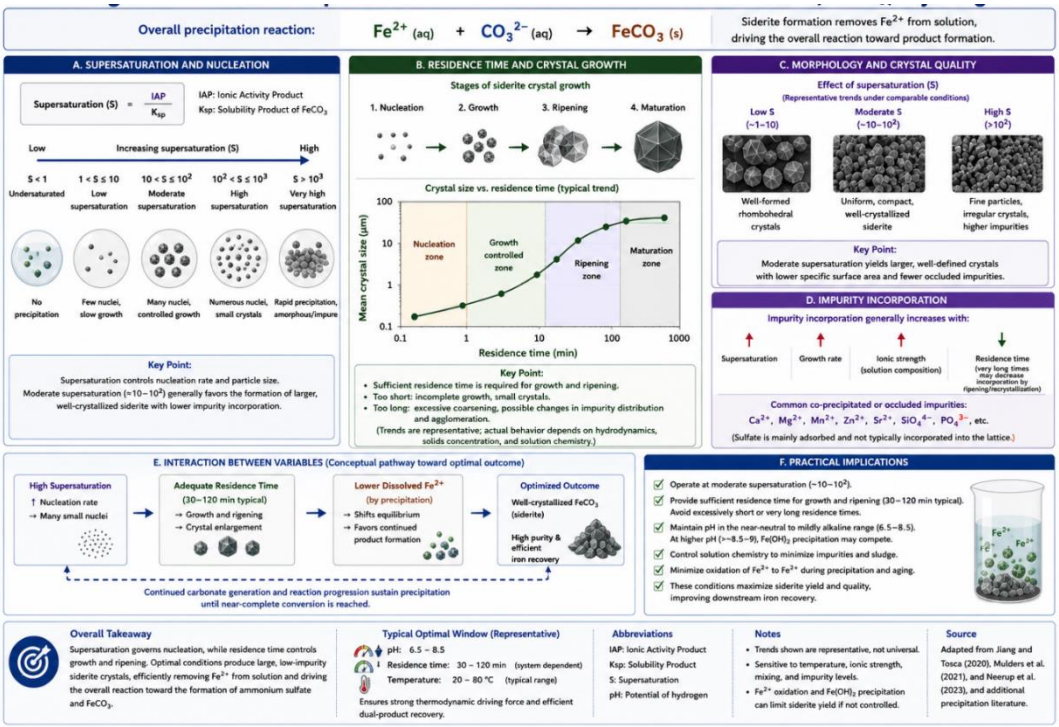

Figure 5. Conceptual influence of supersaturation, pH, residence time, and impurity concentration on ferrous carbonate nucleation, crystal growth, and filtration performance. Adapted from Mulders et al. (2021), Neerup et al. (2023), and Grengs et al. (2024).

Figure 6 illustrates the trade-off between precipitation rate and product quality. High supersaturation may maximize instantaneous precipitation but often generates finer particles. Lower supersaturation generally favors larger crystals and improved solid-liquid separation.

Solid-Liquid Separation

After precipitation, efficient recovery of ferrous carbonate is crucial for process economics. Several separation methods, such as gravity settling, thickening, filtration, centrifugation, and combinations, are applicable.

Filtration is the most practical industrial solution because siderite has a high density (around 3.9–4.0 g/cm³). Filtration rates vary due to particle size and solids loading. Coarse crystals form permeable, low-moisture filter cakes, while fine precipitates create resistant cakes.

Moisture control is particularly important because excess water increases drying requirements and affects downstream reduction performance. Industrial filter cakes are generally targeted to moisture contents below 15–20 wt.% prior to drying operations.

The literature indicates that crystal growth control frequently has a greater influence on filtration performance than the selection of filtration equipment itself. Therefore, optimization of precipitation conditions should be considered an integral part of the recovery process rather than a separate operation.

Drying and Product Stabilization

After filtration, ferrous carbonate typically requires drying before storage or further processing. Drying temperatures must be carefully selected because excessively high temperatures may initiate premature decomposition of siderite.

Most industrial drying operations would likely operate below 150–200 °C. At these temperatures, moisture removal can be achieved while minimizing the risk of decomposition. Rotary dryers, fluidized-bed dryers, tray dryers, and vacuum dryers may all be considered depending on plant scale and product specifications.

Storage conditions also require attention. Exposure to oxygen and moisture may gradually alter product composition through oxidation reactions. Consequently, enclosed storage systems and controlled atmospheres may be desirable for long-term preservation of product quality.

Critical Assessment and Remaining Challenges

Although ferrous carbonate precipitation is thermodynamically favorable, several challenges remain insufficiently addressed in the literature.

First, most published studies focus on relatively pure laboratory solutions. Industrial liquors typically contain complex impurity mixtures that may affect nucleation behavior and product purity.

Second, limited information is available regarding large-scale crystallizer design for siderite recovery. Most investigations remain confined to batch laboratory systems.

Third, interactions between precipitation conditions and downstream hydrogen reduction have received little attention. Crystal morphology, impurity content, and particle size

distribution may significantly influence reduction kinetics and final powder properties.

These knowledge gaps suggest that future work should focus not only on maximizing precipitation efficiency but also on understanding how precipitation conditions affect the entire process chain. This perspective becomes particularly important because ferrous carbonate serves as the intermediate linking sulfate recovery to powder-metallurgy iron production.

The next section examines the second major product generated by the process: ammonium sulfate. Particular attention is given to crystallization behavior, fertilizer specifications, product quality requirements, and market opportunities.

Ammonium Sulfate Recovery and Applications

While ferrous carbonate represents the iron-recovery component of the proposed process, ammonium sulfate constitutes the sulfate-recovery component and is potentially the first commercial product generated. Unlike many waste treatment technologies that produce secondary residues with uncertain market value, ammonium sulfate is a globally traded fertilizer with established production, distribution, and application infrastructure.

Global ammonium sulfate use is around 20–25 million tonnes annually, varying with demand and regional policies. It's valuable in sulfur-deficient soils as it provides nitrogen and sulfur. Producing fertilizer-grade ammonium sulfate from ferrous sulfate waste offers a key economic benefit.

Crystallization and Purification

Following precipitation and separation of ferrous carbonate, the remaining solution contains ammonium sulfate as the principal dissolved salt. Product recovery is generally achieved through concentration and crystallization.

Industrial ammonium sulfate crystallization is a mature, widely used method for fertilizer production. It employs evaporative, vacuum, and cooling crystallizers, or combinations thereof, depending on process conditions (Abeyratne et al., 2023; Avşar & Ertunç, 2025).

The principal objective is to obtain crystals with suitable size distribution, low impurity content, and acceptable handling characteristics. Crystal size is particularly important because excessive fines can lead to dust generation during storage and transportation.

Several factors influence crystallization performance:

- ammonium sulfate concentration;
- temperature profile;
- evaporation rate;
- impurity concentration;
- residence time;
- seeding strategy.

In the proposed process, residual dissolved metals represent the most important purification challenge. Depending on the composition of the original ferrous sulfate solution, traces of manganese, magnesium, aluminum, zinc, copper, or calcium may remain in solution after siderite precipitation.

Table 8 summarizes typical ammonium sulfate product requirements and their implications for fertilizer applications.

Table 8. Typical quality specifications for fertilizer-grade ammonium sulfate and implications for product commercialization. Adapted from Abeyratne et al. (2023), Avşar and Ertunç (2025), Costamagna et al. (2020), Kaljunen et al. (2021), and Koivisto et al. (2023).

Parameter	Typical Specification	Industrial Relevance
Ammonium sulfate purity	> 98–99 wt.%	Fertilizer quality
Nitrogen content	20–21 wt.%	Agronomic value
Sulfur content	23–24 wt.%	Agronomic value
Moisture	< 1 wt.%	Storage stability
Particle size	1–4 mm	Handling performance
Heavy metals	Regulatory dependent	Market acceptance
Bulk density	900–1200 kg/m³	Storage and transport
Water solubility	High	Agricultural efficiency

Table 8 shows that the quality needs for ammonium sulfate are simpler than those for many specialty chemicals, so purification may be less strict than for high-purity metallurgical products.

Product Specifications and Market Requirements

Ammonium sulfate occupies a unique position among nitrogen fertilizers because it supplies both nitrogen and sulfur. The product contains approximately 21 wt.% nitrogen and 24 wt.% sulfur, making it particularly useful in regions where sulfur deficiency limits agricultural productivity.

Commercial prices vary by region, transportation, sulfur markets, and fertilizer demand. From 2020–2025, bulk ammonium sulfate generally ranged from USD 100 to USD 350 per tonne, with temporary deviations during market instability.

This economic value is crucial when evaluating the process. Unlike conventional ferrous sulfate disposal, which incurs costs, ammonium sulfate production generates revenue that offsets expenses for precipitation, filtration, and reduction. However, not all ammonium sulfate markets are equally accessible. Agricultural applications generally tolerate moderate impurity levels, whereas industrial-grade ammonium sulfate may require stricter specifications. Therefore, market selection should be considered during process design.

A recurring issue involves balancing purification costs and product value. Studies show excessive purification can raise costs without proportional revenue gains. Hence, optimal quality depends on the target market, not maximum purity (Costamagna et al., 2020; Koivisto et al., 2023).

Comparison with Conventional Ammonium Sulfate Production Routes

The proposed process differs from traditional ammonium sulfate methods, which usually start with sulfuric acid and ammonia, whereas this approach begins with ferrous sulfate and urea.

This distinction has implications. Conventional production focuses on fertilizer manufacturing, while the proposed route also produces ferrous carbonate. Figure 7 compares major routes.

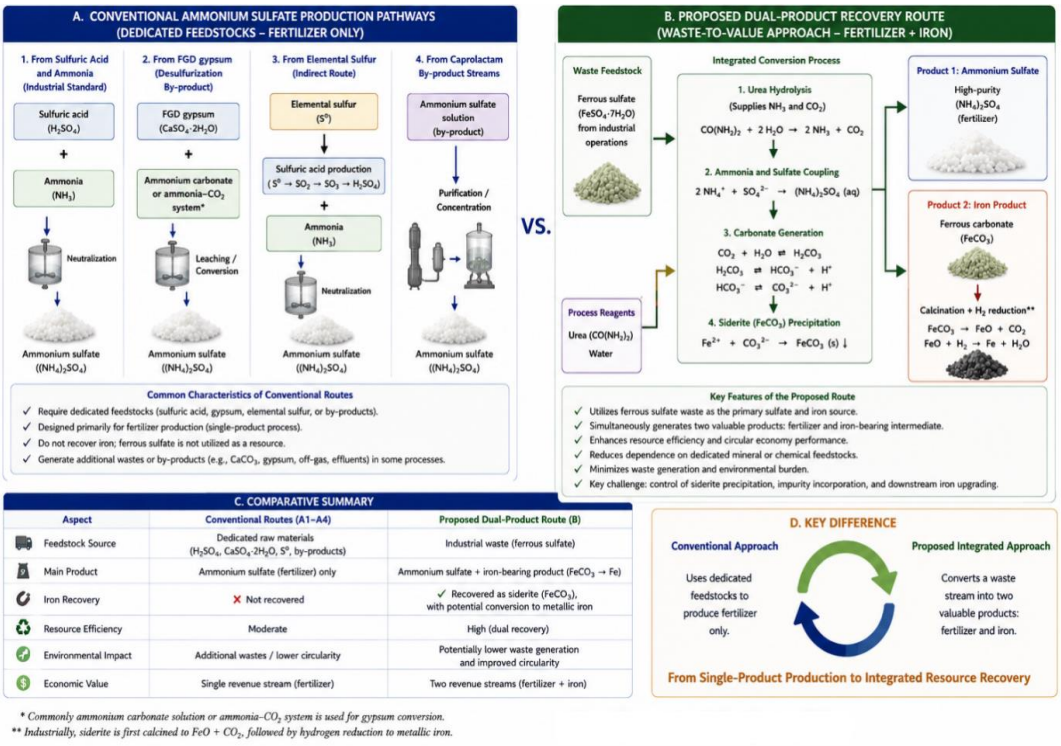

Figure 6. Comparison of conventional ammonium sulfate production pathways and the proposed dual-product recovery route. Adapted from Costamagna et al. (2020), Kaljunen et al. (2021), Koivisto et al. (2023), and Avşar and Ertunç (2025).

Figure 7 highlights a key difference between traditional and integrated approaches. Conventional technologies generally require dedicated feedstocks to produce fertilizer. By contrast, the proposed route utilizes a waste stream as the sulfate source while simultaneously recovering iron.

This dual-product characteristic may improve overall process economics because revenue generation is not entirely dependent on fertilizer markets. If ammonium sulfate prices decline, iron powder production may continue providing economic support. Conversely, fluctuations in iron powder markets may be partially offset by fertilizer sales.

Critical Assessment and Industrial Opportunities

The production of ammonium sulfate from ferrous sulfate solutions offers several advantages, including established markets, mature crystallization technology, and relatively simple product specifications. Nevertheless, several challenges remain.

First, the economic viability of the route depends on local fertilizer markets and transportation logistics. Fertilizers are relatively low-value bulk commodities, making transportation costs important.

Second, impurity management is crucial when processing complex liquors, as ferrous sulfate compositions vary and impurities can build up in ammonium sulfate. Third, few studies have explored optimizing both ammonium sulfate and ferrous carbonate quality simultaneously, since conditions beneficial for one may not suit the other.

Despite these limitations, ammonium sulfate recovery represents one of the strongest aspects of the proposed

process. The existence of a mature market substantially reduces commercialization risks compared with many waste valorization technologies that rely on niche applications.

The discussion shows the first product has clear commercial value. The next part explores the conversion of ferrous carbonate to metallic iron powder via hydrogen reduction, which is crucial for meeting powder metallurgy quality standards.

Hydrogen Reduction of Siderite

The conversion of ferrous carbonate into metallic iron is the second major value-stage of the process. While ammonium sulfate recovery yields an immediate product, transforming siderite into powder-metallurgy iron substantially boosts the iron's value. This step also sets the process apart from many ferrous sulfate technologies that end at intermediate iron compounds.

Hydrogen reduction is an alternative to carbon-intensive ironmaking, emitting water vapor rather than CO or solid carbon. When sourced from renewable sources, it greatly reduces greenhouse gas emissions (Fan et al., 2025; Souza Filho et al., 2022).

Thermal Decomposition of Ferrous Carbonate

Before metallic iron can be produced, ferrous carbonate undergoes thermal decomposition. The decomposition pathway is influenced by temperature, atmosphere composition, heating rate, and particle characteristics.

The simplified decomposition reaction is:
$FeCO_3 \rightarrow FeO + CO_2$

Thermogravimetric studies indicate that siderite decomposition commonly begins between 350 and 450 °C and becomes increasingly significant above approximately 450–500 °C. However, reported values vary depending on crystal morphology, particle size, impurity content, and gas atmosphere (Kądziołka-Gaweł et al., 2023; Zhang et al., 2021).

Several studies show that decomposition differs between natural siderite ores and synthetic ferrous carbonate. Natural ores contain impurities such as silicates, carbonates, sulfides, and oxides, which affect decomposition temperatures and gas release. Precipitated siderite from aqueous systems usually has higher purity and consistent thermal behavior (Zhang et al., 2022; Zhu et al., 2023).

The decomposition stage is important not only because it generates iron oxide intermediates but also because it influences subsequent reduction kinetics. Porosity generated during CO_2 evolution frequently improves gas penetration and enhances hydrogen accessibility to reaction sites.

Table 8 summarizes the thermodynamic parameters calculated for hydrogen reduction of ferrous carbonate.

Table 9. Thermodynamic parameters calculated using HSC Chemistry for hydrogen reduction of ferrous carbonate. Adapted from Li et al. (2021), Kleiber et al. (2024), and HSC Chemistry simulations performed for the present review.

T (°C)	ΔH (kcal/mol)	ΔS (cal/mol·K)	ΔG (kcal/mol)	K	Log K
0	25.240	49.618	11.687	4.45×10^{-10}	-9.351
100	24.849	48.406	6.786	1.06×10^{-4}	-3.975
200	24.346	47.218	2.005	1.19×10^{-1}	-0.926
300	23.726	46.032	-2.658	1.03×10^{1}	1.013
400	22.990	44.852	-7.202	2.18×10^{2}	2.338
500	22.146	43.684	-11.628	1.94×10^{3}	3.287
600	21.208	42.544	-15.940	9.77×10^{3}	3.990
700	20.214	41.467	-20.139	3.34×10^{4}	4.523
800	19.173	40.451	-24.237	8.64×10^{4}	4.936
900	17.688	39.130	-28.217	1.81×10^{5}	5.257
1000	15.997	37.755	-32.071	3.20×10^{5}	5.506

Table 8 shows a clear thermodynamic transition: at low temperatures, a positive Gibbs free energy indicates that reduction is unfavorable, but ΔG turns negative near 250–300 °C, with the equilibrium constant then rising rapidly.

This behavior differs from ferrous sulfate conversion. While precipitation is favorable across a range of temperatures, hydrogen reduction requires higher temperatures, though still lower than those of many conventional ironmaking processes.

Thermodynamics of Hydrogen Reduction

The HSC results indicate that hydrogen reduction becomes increasingly favorable as temperature rises. At 300 °C, the equilibrium constant already exceeds unity. At 600 °C, K approaches 10^4, and the value continues to increase at higher temperatures.

The thermodynamic behavior can be understood from the entropy contribution associated with gas-phase reactions. As temperature increases, the TΔS term becomes increasingly

significant, driving Gibbs free energy toward more negative values.

This observation has important practical implications. It shows complete reduction can be achieved below 1000 °C and integrated with simple furnace tech. It also suggests producing metallic iron powders with less energy than some conventional methods.

However, thermodynamic favorability alone doesn't ensure rapid reduction. Studies show that reaction kinetics can become rate-limiting at lower temperatures, despite equilibrium favoring the formation of metallic iron (Li et al., 2021; Miškovičová et al., 2024).

Figure 8 summarizes the effect of temperature on the thermodynamics of reduction.

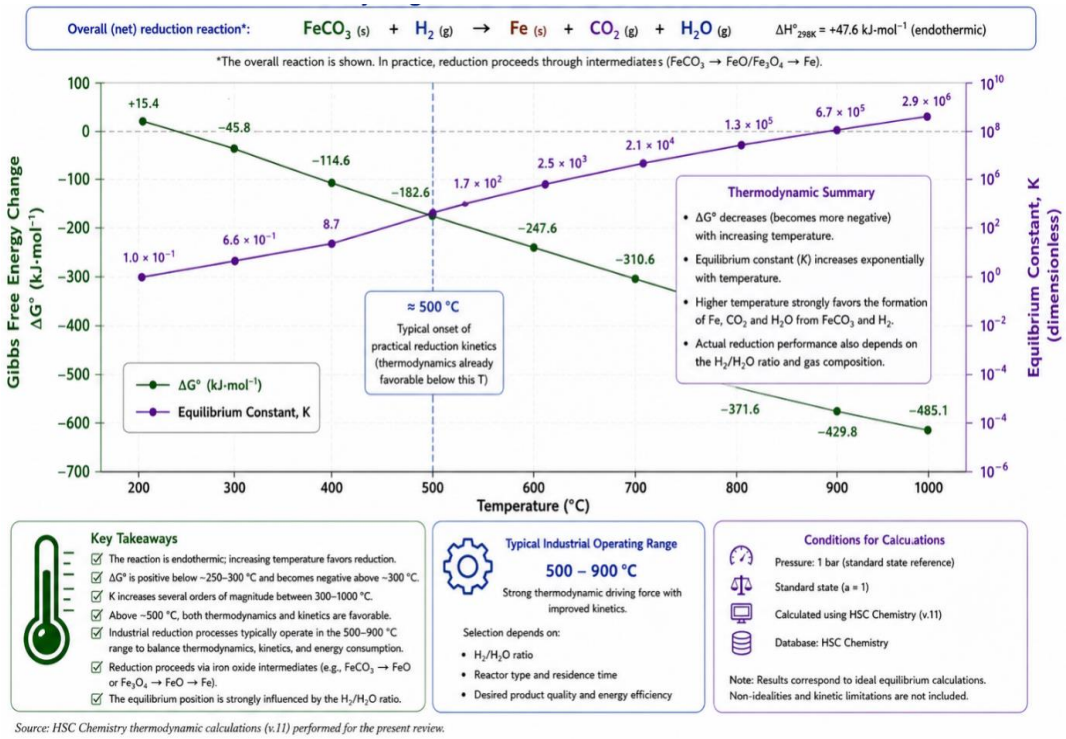

Figure 7. Temperature dependence of Gibbs free energy and equilibrium constant for hydrogen reduction of ferrous carbonate. Adapted from HSC Chemistry simulations performed for the present review.

Figure 8 highlights that temperatures above approximately 500 °C provide particularly strong thermodynamic driving force. Consequently, many industrial reduction processes operate at 500–800 °C to balance thermodynamic and kinetic considerations with energy consumption.

Reduction Kinetics and Mechanisms

Although thermodynamics determines reaction feasibility, kinetics determines production rate and reactor size. The reduction of ferrous carbonate generally proceeds through multiple stages involving decomposition, nucleation of metallic iron, growth of reduced regions, and diffusion of gaseous species.

Several authors have proposed shrinking-core, nucleation-growth, and mixed-control models for describing reduction behavior. The dominant mechanism depends on particle size, porosity, temperature, and gas composition (Hessels et al., 2022; Hessels et al., 2023).

At lower temperatures, surface chemical reactions often dominate. As temperature increases, diffusion through porous product layers may become increasingly important. The formation of metallic iron can either accelerate or hinder reduction depending on the resulting microstructure.

A recurring contradiction in the literature concerns the optimum reduction temperature. Some studies report maximum efficiency near 600 °C, whereas others favor temperatures above 700 °C. These differences frequently arise from variations in particle size, hydrogen purity, gas flow rate, and feed composition rather than fundamental disagreements regarding reduction mechanisms (Loder et al., 2022; Ma et al., 2022).

Static-Bed and Tray-Furnace Reduction

For the process considered in this review, static-bed and tray furnaces appear particularly attractive because they are compatible with relatively coarse precipitated siderite particles and moderate production capacities.

In static-bed systems, ferrous carbonate is loaded into trays or fixed beds through which hydrogen flows continuously. Reduction proceeds progressively as hydrogen penetrates the particle bed. The simplicity of these systems reduces mechanical complexity and facilitates operation under controlled atmospheres.

Typical operating parameters reported in the literature include:

- Temperature: 500–800 °C
- Hydrogen purity: >95%
- Residence time: 1–8 h
- Bed depth: 20–200 mm
- Pressure: atmospheric to slightly elevated

Tray furnaces offer similar advantages while providing greater flexibility for batch production. Such systems are widely used in powder metallurgy and heat-treatment industries and therefore benefit from extensive industrial experience (Kleiber et al., 2024; Zhou et al., 2026).

Compared with fluidized beds, static-bed systems generally exhibit lower gas utilization efficiency but simpler operation and lower capital requirements. Consequently, they may be particularly attractive for small- to medium-scale applications.

Influence of H_2/H_2O Ratio

The ratio between hydrogen and water vapor strongly influences reduction performance. Water vapor is a direct reaction product and therefore affects equilibrium conditions.

Higher H_2/H_2O ratios generally favor reduction by shifting equilibrium toward metallic iron. Conversely, excessive water vapor concentrations may slow reduction and, under certain conditions, promote partial reoxidation.

Several studies have demonstrated that gas recycling systems require careful control of water vapor accumulation. Although recycling improves hydrogen utilization efficiency, insufficient moisture removal may reduce overall process performance (Fan et al., 2025; Souza Filho et al., 2022).

Critical Assessment and Industrial Outlook

The literature strongly supports the thermodynamic feasibility of hydrogen reduction of ferrous carbonate. The HSC calculations presented in Table 8 demonstrate that temperatures above approximately 300 °C provide favorable equilibrium conditions, while temperatures above 500 °C provide strong thermodynamic driving force.

Nevertheless, several challenges remain. Most published studies focus on iron oxides rather than precipitated ferrous carbonate. Consequently, relatively limited information is available regarding the reduction behavior of siderite produced from hydrometallurgical process streams.

Another important uncertainty concerns impurity effects. Elements incorporated during precipitation may influence reduction kinetics, particle morphology, and final powder properties. These interactions remain insufficiently studied.

Despite these limitations, hydrogen reduction appears to be one of the most promising pathways for upgrading recovered siderite into a high-value metallurgical product. The resulting metallic powder may serve applications in powder metallurgy, additive manufacturing, magnetic materials, and specialty iron applications.

The next section examines the characteristics, performance requirements, and market opportunities of iron produced by powder metallurgy from ferrous carbonate intermediates.

Powder Metallurgy Iron from Ferrous Carbonate

The economic attractiveness of the proposed process depends on efficient conversion of ferrous sulfate and hydrogen reduction, and on the commercial value of the resulting iron powder. Powder metallurgy (PM) is a major consumer of iron powder, serving the automotive, machinery, magnetic, chemical, and structural industries. Transforming waste-derived intermediate into PM-grade feedstock enhances the process's value.

Global iron powder production exceeds several million tonnes annually. Conventional manufacturing routes include water atomization, gas atomization, sponge iron reduction, carbonyl decomposition, and electrolytic production. Each technology produces powders with distinct particle morphologies, purity levels, and cost structures (Alghtani et al., 2022; Gan et al., 2024).

The route proposed in this review shares several characteristics with conventional sponge iron powder production but differs in its feedstock origin. Instead of starting from iron ore concentrates or mill scale, the process utilizes ferrous carbonate recovered from industrial waste streams.

Iron Powder Characteristics

The quality requirements for powder metallurgy applications vary considerably according to the intended use. Structural PM components generally prioritize compressibility and green strength, whereas magnetic materials and specialty applications may require higher purity and tighter particle-size control.

Hydrogen reduction frequently produces porous iron particles characterized by high surface area and good compressibility. Such characteristics are advantageous for conventional press-and-sinter operations because they facilitate mechanical interlocking during compaction.

Several powder properties are particularly important:

- Chemical purity
- Apparent density
- Flowability
- Particle size distribution
- Compressibility
- Green density
- Sinterability

The influence of these parameters on commercial applications is summarized in Table 10.

Table 10. Typical powder metallurgy iron powder specifications and performance requirements. Adapted from Alghtani et al. (2022), Gan et al. (2024), Gan et al. (2025), Hong et al. (2026), and Yao et al. (2021).

Property	Typical Range	Importance
Iron purity	95–99.9 wt.%	Product quality
Particle size	20–300 μm	Flowability and compaction
Apparent density	2.0–3.5 g/cm³	Die filling behavior
Green density	6.5–7.3 g/cm³	Mechanical performance
Oxygen content	<0.5 wt.%	Sinterability
Carbon content	<0.1 wt.%	Metallurgical control
Compressibility	High	PM processing
Surface area	Process dependent	Reactivity

Table 10 shows that hydrogen-reduced iron powders can meet many industrial needs if impurities are well controlled, especially since the process uses secondary resources rather than traditional iron ore.

Powder Morphology and Metallurgical Performance

Particle morphology strongly influences powder behavior during compaction and sintering. Atomized powders typically exhibit irregular shapes resulting from rapid solidification, whereas hydrogen-reduced powders often retain porous structures inherited from their precursor materials.

The reduction of ferrous carbonate may generate highly porous particles because CO_2 evolution during decomposition creates internal voids. Subsequent reduction to metallic iron can preserve part of this porosity, producing powders with favorable compressibility characteristics.

However, excessive porosity may also present disadvantages. High surface area increases susceptibility to oxidation during storage and handling. Furthermore, extremely porous powders may exhibit lower apparent density, increasing transportation and storage costs.

The literature indicates that optimum powder characteristics depend strongly on the target application. Structural PM components generally benefit from moderate porosity and high compressibility, whereas magnetic applications often prioritize chemical purity and a controlled particle-size distribution (Gan et al., 2025; Hong et al., 2026).

A further consideration concerns residual impurities originating from the precipitation stage. Elements such as manganese, calcium, magnesium, aluminum, or silicon may remain within the reduced powder. Depending on concentration levels, these elements may either improve or impair final performance.

Comparison with Conventional Iron Powder Production Routes

Several commercial technologies currently dominate iron powder production. Each route presents specific advantages and limitations.

Figure 9 compares the principal production pathways.

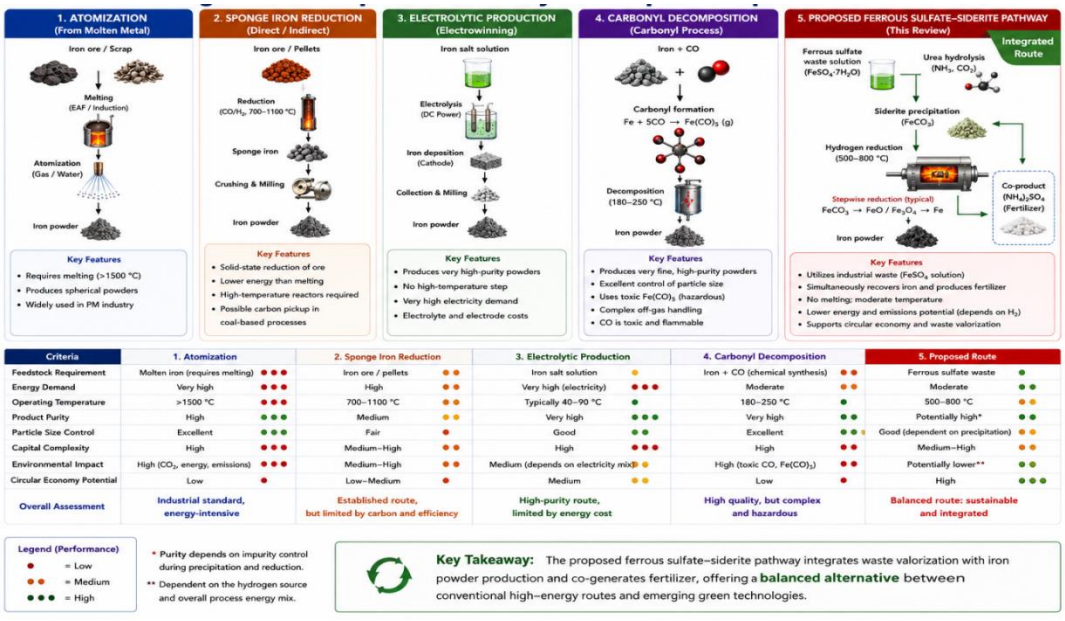

Figure 8. Comparison of major iron powder production routes, including atomization, sponge iron reduction, electrolytic production, carbonyl decomposition, and the proposed ferrous sulfate–siderite pathway. Adapted from Wendel et al. (2020a), Wendel et al. (2020b), Hu et al. (2025), Wu et al. (2023), Tang et al. (2022), and Zhou et al. (2025).

Figure 9 highlights that the proposed route occupies a position between conventional sponge iron production and waste valorization technologies. Unlike atomization routes, it does not require molten metal. Unlike electrolytic routes, it does not require high electrical energy consumption. Unlike carbonyl processes, it avoids handling toxic carbonyl intermediates.

The production route strongly influences the cost structure, product quality, energy consumption, environmental footprint, and industrial applicability of iron powders. Conventional technologies such as atomization, sponge iron reduction, electrolytic production, and carbonyl decomposition have been extensively commercialized, each offering distinct advantages and limitations. In the context of the present review, it is important to position the proposed ferrous sulfate–siderite route relative to these established technologies. Table 11 compares the major iron powder production pathways in terms of feedstock requirements, achievable purity, and relative capital and operating costs.

Table 11. Comparison of major iron powder production routes based on feedstock characteristics, product purity, and relative economic requirements. Adapted from Wendel et al. (2020a), Wendel et al. (2020b), Tang et al. (2022), Wu et al. (2023), Hu et al. (2025), and Zhou et al. (2025).

Route	Feedstock	Typical Purity	Relative CAPEX	Relative OPEX
Water atomization	Molten iron	High	High	Moderate
Gas atomization	Molten iron	Very high	Very high	High
Sponge iron reduction	Iron ore	High	Moderate	Moderate
Electrolytic	Iron salts	Very high	High	High
Carbonyl	Iron carbonyl	Ultra-high	Very high	Very high
Proposed route	$FeSO_4$ waste	Potentially high	Moderate	Moderate

Table 11 highlights the unique position of the proposed ferrous sulfate–siderite route among established iron powder methods. Atomization produces high-quality powders but requires molten metal and high energy input. Sponge iron reduction is cheaper but relies on primary iron ore. Electrolytic and carbonyl routes achieve high purity but are costly and involve hazardous intermediates. The proposed route uses ferrous sulfate waste, avoids molten metal and toxic compounds, and creates ammonium sulfate as a co-product. It offers a good balance of product quality, resource efficiency, and circular economy benefits, though pilot validation and detailed economic analysis are still needed.

The proposed route benefits from low-cost feedstock because ferrous sulfate is often considered waste or a low-value by-product. Consequently, feedstock cost may be substantially lower than that associated with conventional ore-based routes.

However, the route introduces additional process steps, including urea conversion, siderite precipitation, filtration, and drying. Therefore, the economic advantage ultimately depends on the balance between feedstock savings and additional processing costs.

Market Opportunities

The powder metallurgy industry continues to expand despite increasing competition from additive manufacturing and advanced forming technologies. Automotive components remain the largest market segment, although demand for soft magnetic materials, filters, friction materials, and specialty powders has also increased.

Iron powder prices vary considerably depending on purity, particle morphology, and application. Commodity-grade powders may sell for several hundred dollars per tonne, whereas specialty powders may command substantially higher prices.

This price variability creates opportunities for process optimization. For example, lower-purity powders may be suitable for structural applications, whereas additional purification could enable access to higher-value specialty markets.

A particularly interesting opportunity concerns sustainable iron powders. As decarbonization becomes increasingly important, powders produced using hydrogen reduction and waste-derived feedstocks may benefit from environmental advantages not available to conventional production routes.

Critical Assessment

Although the proposed pathway offers significant promise, several uncertainties remain.

First, limited information is available regarding the powder characteristics generated specifically from precipitated ferrous carbonate. Most available reduction studies focus on natural siderite ores or conventional iron oxides.

Second, impurity behavior throughout the complete process chain remains insufficiently understood. The precipitation stage, reduction stage, and powder finishing stage may all influence final product quality.

Third, large-scale demonstration studies remain scarce. Consequently, the relationship between laboratory performance and industrial production remains uncertain.

Nevertheless, the literature strongly suggests that hydrogen reduction of ferrous carbonate can produce iron powders with characteristics that are potentially suitable for powder

metallurgy applications. When combined with the simultaneous production of ammonium sulfate fertilizer, this capability substantially strengthens the economic rationale for the integrated process.

The discussion thus far has focused on the individual products generated by the proposed route. However, evaluating industrial viability requires analysis of the entire process chain. The next section, therefore, examines process integration, circular economy benefits, mass-flow considerations, and environmental implications associated with the simultaneous recovery of fertilizer and metallic powder from ferrous sulfate waste streams.

Integrated Process Assessment and Circular Economy

The previous sections evaluated the individual stages of the proposed process chain, including ferrous sulfate conversion, siderite precipitation, ammonium sulfate recovery, and hydrogen reduction of ferrous carbonate. However, industrial viability ultimately depends on how these stages interact as an integrated system. Process integration is particularly important because the economic and environmental benefits arise from the simultaneous generation of two marketable products from a residue that would otherwise require treatment or disposal.

A key advantage of the proposed route is that both major products originate from the same feedstock. Sulfate values are recovered as ammonium sulfate fertilizer, while iron values are recovered as powder metallurgy feedstock. Consequently, the process avoids the common limitation observed in many waste treatment technologies, where recovery of one component generates a secondary residue requiring additional management.

Integrated Mass Flow Concept

The integrated process begins with a ferrous sulfate solution generated by hydrometallurgical, pickling, titanium dioxide, or related industrial operations. Urea is introduced as the nitrogen and carbonate precursor. Following hydrolysis and precipitation, the process generates two primary streams:
Solid ferrous carbonate.
Ammonium sulfate solution.

The ferrous carbonate stream is filtered, dried, and reduced using hydrogen to produce metallic iron powder. Simultaneously, the ammonium sulfate solution is concentrated and crystallized to produce fertilizer-grade ammonium sulfate.

Before discussing environmental implications, the overall process concept is summarized in Figure 10.

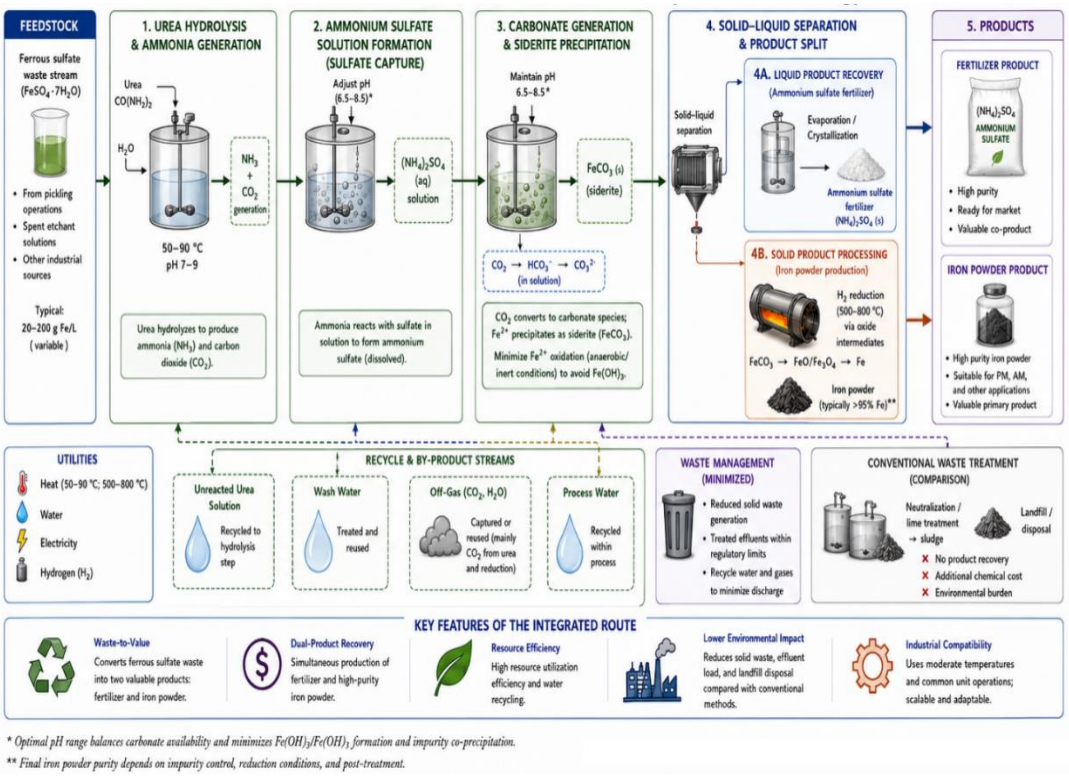

Figure 9. Integrated conceptual flowsheet for conversion of ferrous sulfate waste streams into ammonium sulfate fertilizer and powder metallurgy iron. Adapted from Harvey et al. (2020), Jiang and Tosca (2020), Fan et al. (2025), and developed by the authors.

Figure 10 illustrates the fundamental distinction between the proposed route and conventional waste treatment strategies. Instead of converting ferrous sulfate into a disposal residue, the process transforms both sulfate and iron into commercially valuable products.

For illustration purposes, a simplified mass-balance framework is presented in Table 12.

Table 12. Simplified comparison between conventional ferrous sulfate disposal and integrated dual-product recovery. Adapted from Branca et al. (2020), Vilaça et al. (2022), Swain et al. (2022), and developed by the authors.

Aspect	Conventional Disposal	Proposed Integrated Route
Sulfate value	Lost	Recovered as ammonium sulfate
Iron value	Lost or partially recovered	Recovered as iron powder
Waste generation	High	Significantly reduced
Landfill requirement	Often necessary	Potentially minimized
Revenue streams	None or limited	Two independent products
Circular economy potential	Low	High
Carbon reduction potential	Limited	Moderate to high
Resource efficiency	Low	High

Table 12 demonstrates that the proposed route addresses two objectives simultaneously: waste minimization and resource recovery. This dual benefit is uncommon among conventional ferrous sulfate treatment technologies.

Environmental Benefits

The environmental advantages of the proposed process extend beyond simple waste reduction. Conventional management strategies frequently convert dissolved ferrous sulfate into hydroxide sludges, gypsum-rich residues, or stabilized landfill materials. Although these approaches may satisfy regulatory requirements, they generally do not recover material value.

By contrast, the proposed route promotes recovery of both iron and sulfate. Consequently, fewer raw materials are required to produce equivalent quantities of fertilizer and iron powder elsewhere in the industrial system.

Several authors have emphasized that resource recovery often provides greater environmental benefits than waste stabilization because it reduces demand for primary raw materials (Akinwekomi et al., 2020; Kazanc et al., 2024). In the present case, recovery of sulfate reduces dependence on conventional ammonium sulfate production routes, while recovery of iron reduces dependence on virgin iron feedstocks.

A further environmental benefit arises from the potential reduction of landfill requirements. Disposal costs and long-term environmental liabilities associated with ferrous sulfate residues remain significant concerns in many jurisdictions. Transforming these residues into marketable products directly addresses this issue.

Carbon Footprint and Green Hydrogen Opportunities

The carbon footprint of the proposed process depends strongly on hydrogen production methods. If hydrogen is produced from fossil fuels without carbon capture, environmental benefits may be partially offset by upstream emissions.

However, when green hydrogen is available, the reduction stage offers substantial opportunities for emission reduction. Unlike carbon-based reduction systems, hydrogen reduction produces water vapor rather than carbon monoxide as the principal reaction product.

Several recent studies have identified hydrogen metallurgy as one of the most promising pathways for decarbonizing iron production (Fan et al., 2025; Souza Filho et al., 2022). The present process could potentially benefit from these developments because the reduction stage operates at temperatures substantially lower than those employed in conventional blast furnace operations.

The carbon intensity associated with urea production must also be considered. Nevertheless, because urea simultaneously supplies nitrogen and carbonate species, its utilization may reduce the need for additional reagents and partially offset environmental impacts.

A comprehensive life-cycle assessment remains beyond the scope of the present review. However, available evidence suggests that integration of waste-derived feedstocks with hydrogen reduction offers significant potential for reducing environmental burdens relative to conventional disposal practices.

Circular Economy Perspective

The proposed route aligns closely with circular economy principles because it transforms a residue into multiple useful products. Instead of viewing ferrous sulfate as a waste requiring management, the process treats it as a secondary resource containing recoverable sulfate and iron values.

From a circular economy perspective, the process exhibits several favorable characteristics:

- Recovery of multiple components.
- Reduction of landfill dependence.
- Potential reduction of primary resource consumption.
- Creation of multiple revenue streams.
- Compatibility with low-carbon hydrogen technologies.

However, circular economy benefits should not be assumed automatically. Economic viability, product quality, logistics, and market demand remain essential considerations. A technically successful recovery process may still fail

commercially if product specifications cannot be achieved or if transportation costs exceed product value.

This observation highlights a recurring theme throughout the review: thermodynamic feasibility is necessary but not sufficient. Successful implementation requires simultaneous consideration of chemistry, engineering, economics, and market conditions.

Critical Assessment of Process Integration

The integrated route presents several important strengths. First, each major stage is thermodynamically favorable under practical operating conditions. Second, both principal products have established markets. Third, the process utilizes relatively simple chemistry and widely available reagents.

Nevertheless, several uncertainties remain. Large-scale demonstrations are currently lacking. Impurity accumulation throughout the process chain remains insufficiently understood. Product quality requirements may vary substantially among industries and regions. Furthermore, the economics of hydrogen supply remain highly location dependent.

Despite these challenges, the combined evidence suggests that the proposed process represents a promising example of industrial symbiosis and waste valorization. The ability to generate fertilizer and metallic powder simultaneously distinguishes it from most existing ferrous sulfate management technologies.

The final technical section of this review examines the principal techno-economic barriers that must be overcome before industrial implementation can occur. Particular attention is given to hydrogen consumption, urea requirements, purification costs, and scale-up challenges.

Techno-Economic Challenges and Research Needs

The preceding sections demonstrate that the proposed process is thermodynamically feasible and can generate two commercially relevant products. Nevertheless, industrial implementation depends on factors that extend beyond reaction chemistry. Capital investment, operating costs, product quality requirements, hydrogen availability, and process scale all influence economic viability. Consequently, a critical assessment of these challenges is essential before considering commercial deployment.

A recurring issue in the literature is the tendency to evaluate individual process stages independently. While such studies provide valuable scientific information, they often overlook interactions among precipitation, crystallization, reduction, and product purification. These interactions may significantly affect overall economics.

Urea Consumption and Reagent Costs

Urea is one of the least expensive nitrogen-containing industrial chemicals. Global production exceeds 180 million tonnes annually, and international prices commonly fluctuate between approximately USD 250 and USD 600 per tonne depending on energy markets, natural gas prices, and fertilizer demand.

The stoichiometry of the proposed process indicates that urea performs two simultaneous functions:

- nitrogen source for ammonium sulfate formation;
- carbonate source for siderite precipitation.
- This dual functionality distinguishes urea from conventional process alternatives, where ammonia and carbonate reagents are often supplied separately.

However, actual urea consumption may exceed stoichiometric requirements due to incomplete hydrolysis, side reactions, and process inefficiencies. Therefore, optimization of hydrolysis conditions remains an important research priority.

Hydrogen Consumption and Energy Requirements

Hydrogen availability represents one of the most important factors affecting process economics. Although hydrogen reduction offers significant environmental advantages, hydrogen remains more expensive than conventional reducing agents in many regions.

The reduction reaction:

$$FeCO_3 + H_2 \rightarrow Fe + CO_2 + H_2O$$

requires approximately 17.3 kg of hydrogen per tonne of iron produced on a stoichiometric basis. Actual consumption is generally higher because industrial systems require excess hydrogen to maintain favorable reduction conditions and compensate for gas-distribution inefficiencies.

- Current hydrogen prices vary widely:
- Gray hydrogen: approximately USD 1–3/kg
- Blue hydrogen: approximately USD 2–5/kg
- Green hydrogen: approximately USD 3–10/kg

As a result, hydrogen cost may become one of the dominant operating expenses for the reduction stage.

Nevertheless, this challenge must be evaluated within the broader context of decarbonization. Many jurisdictions are investing heavily in low-carbon hydrogen infrastructure, and future cost reductions are widely anticipated (Fan et al., 2025; Zhou et al., 2025).

Product Purification and Quality Control

Product quality requirements represent another major challenge.

For ammonium sulfate, agricultural markets generally tolerate moderate impurity levels. Consequently, purification requirements may be relatively manageable.

The situation is more complex for iron powder. Powder metallurgy applications often impose strict specifications regarding:

- oxygen content;
- carbon content;
- sulfur content;
- particle-size distribution;
- apparent density;
- compressibility.

Impurities introduced during precipitation may therefore influence the commercial value of the final powder. Additional purification steps may be required in some applications, increasing both capital and operating costs.

This issue highlights an important knowledge gap in the current literature. Most published studies evaluate precipitation efficiency or reduction efficiency independently, whereas relatively few examine complete impurity pathways through the entire process chain.

Scale-Up Challenges

Scale-up remains one of the least explored aspects of the proposed route.

Most studies involving ferrous carbonate precipitation have been performed at laboratory scale using batch reactors. Similarly, many hydrogen reduction investigations employ small fixed-bed systems or thermogravimetric analyzers.

Industrial implementation introduces additional complexities:

- mixing limitations;
- heat-transfer constraints;
- gas-distribution effects;
- particle segregation;
- filtration bottlenecks;
- crystallization control.

These factors may significantly influence performance and product quality.

The challenge is particularly important because the process contains both liquid-phase and gas-solid operations. Successful integration therefore requires expertise from hydrometallurgy, crystallization engineering, powder metallurgy, and hydrogen metallurgy.

Table 13 summarizes the principal techno-economic challenges identified throughout the review.

Table 13. Principal techno-economic challenges associated with industrial implementation of the proposed dual-product recovery route. Adapted from Fan et al. (2025), Kazanc et al. (2024), Kleiber et al. (2024), Rongwong et al. (2022), and Furmanski et al. (2025).

Challenge	Impact Level	Main Consequence	Research Priority
Hydrogen cost	High	Increased OPEX	High
Product purification	High	Reduced market value	High
Scale-up uncertainty	High	Commercialization risk	High
Urea utilization efficiency	Moderate	Reagent consumption	Moderate
Crystallization control	Moderate	Product quality variation	Moderate
Gas recycling	Moderate	Energy consumption	Moderate
Impurity management	High	Product contamination	High
Market fluctuations	Moderate	Revenue uncertainty	Moderate

Table 13 shows that the most significant challenges are associated with hydrogen supply, impurity management, and scale-up. These issues should therefore receive priority attention in future research and pilot-scale development programs.

Research Priorities

Several research directions emerge from the analysis presented in this review.

First, pilot-scale demonstrations are required to validate process integration under realistic operating conditions. Laboratory studies provide valuable mechanistic information but cannot fully capture scale-dependent phenomena.

Second, impurity behavior throughout the complete process chain should be investigated. Understanding impurity partitioning between siderite, ammonium sulfate, and iron powder is essential for predicting product quality.

Third, integrated techno-economic assessments are needed. Such analyses should evaluate capital investment, operating costs, product revenues, and sensitivity to hydrogen and fertilizer prices.

Finally, future studies should explore the use of renewable hydrogen and renewable electricity. These developments could substantially improve the process's environmental performance and strengthen its alignment with circular economy objectives.

The challenges discussed in this section are significant but not insurmountable. In many cases, they resemble those encountered during development of other resource-recovery

technologies that subsequently achieved commercial success. Consequently, the available evidence suggests that the proposed route warrants further investigation beyond laboratory scale.

Conclusions

Ferrous sulfate remains one of the most widely generated sulfate-bearing residues in chemical, metallurgical, and hydrometallurgical industries. Although numerous utilization pathways have been proposed, large quantities continue to be treated as wastes or low-value by-products. This review evaluated an alternative approach based on integrated recovery of sulfate and iron values through production of ammonium sulfate fertilizer and powder metallurgy iron.

The analysis demonstrates that urea-assisted conversion of ferrous sulfate into ammonium sulfate and ferrous carbonate is strongly supported by thermodynamic considerations. HSC calculations indicate favorable Gibbs free energy values and equilibrium constants across practical operating temperatures. The low solubility of ferrous carbonate provides an additional driving force by continuously removing iron from solution and shifting equilibrium toward product formation.

The review further shows that hydrogen reduction of ferrous carbonate is thermodynamically feasible at moderate temperatures. Above approximately 300 °C, reduction becomes favorable, while temperatures above 500 °C provide strong thermodynamic driving force. These conditions are compatible with established furnace technologies commonly used in powder metallurgy and heat-treatment industries.

From a circular economy perspective, the proposed route offers several advantages. It transforms a problematic industrial residue into two commercially valuable products, reduces dependence on disposal practices, and creates opportunities for resource recovery. The existence of established markets for both ammonium sulfate and iron powder further strengthens the industrial relevance of the concept.

Nevertheless, important challenges remain. Product purification, impurity management, hydrogen cost, and process scale-up require additional investigation. Pilot-scale demonstrations and integrated techno-economic assessments are particularly important for evaluating commercial feasibility.

Overall, the available evidence indicates that the proposed dual-product recovery route represents a promising strategy for converting ferrous sulfate waste streams into fertilizer and metallic powder products. Future advances in hydrogen technology, process integration, and resource recovery are likely to further improve its attractiveness as a sustainable industrial solution.

Declarations

Author Contributions

Antonio Clareti Pereira: Conceptualization, Methodology, Literature Investigation, Data Curation, Thermodynamic Analysis, Writing – Original Draft, Writing – Review & Editing.

Funding

The author received no specific funding for this work.

Data Availability Statement

The datasets generated and analyzed during the current study are available from the corresponding author upon reasonable request.

Conflicts of Interest

The author declares no conflicts of interest.

Acknowledgments

The author acknowledges the valuable contributions of researchers whose studies provided the scientific foundation for the present critical review.

References

1. Abbadi, F. Z., Azoulay, K., Moufti, A., Ait Hou, A., & Jemjami, S. (2026). Thermodynamic calculation on the thermal decomposition of different types of calcium carbonates using the computational thermochemistry tool HSC Chemistry. In *Integration of Advanced Systems in Environmental Science and Water Desalination* (1st ed., pp. xx–xx). CRC Press..
2. Abeyratne, W. M. L. K., Bayat, H., et al. (2023). Feasibility of ammonium sulfate recovery from wastewater sludges: Hydrothermal liquefaction pathway vs. anaerobic digestion pathway. *Journal of Environmental Management, 338*, 117786.
3. Agarwal, C., & Pandey, A. K. (2023). Remediation and recycling of inorganic acids and their green alternatives for sustainable industrial chemical processes. *Environmental Science: Advances, 2*(9), 1306–1339. https://doi.org/10.1039/D3VA00112A.
4. Akinwekomi, V., Maree, J. P., Masindi, V., Zvinowanda, C., Osman, M. S., Foteinis, S., Mpenyana-Monyatsi, L., & Chatzisymeon, E. (2020). Beneficiation of acid mine drainage (AMD): A viable option for the synthesis of goethite, hematite, magnetite, and gypsum—Gearing towards a circular economy concept. *Minerals Engineering, 148*, 106204. https://doi.org/10.1016/j.mineng.2020.106204.
5. Alghtani, A. H., Alsharef, M., & Abdel-Aziz, K. (2022). Characterization of iron powder produced by reduction of hot-rolled mill scale in hydrogen gas.

Materials Research, 25, e20210575. https://doi.org/10.1590/1980-5373-MR-2021-0575

6. Avşar, C., & Ertunç, S. (2025). Reaction parameter optimization of ammonium sulfate production from phosphogypsum. *Chemical Industry and Chemical Engineering Quarterly, 31*(1), 61–69. https://doi.org/10.2298/CICEQ231130013A.
7. Avşar, C., Tümük, D., Ertunç, S., & Gezerman, A. O. (2022). A review on ammono-carbonation reactions: Focusing on the Merseburg process. Chemical Review and Letters, 5(1), 83–91. https://doi.org/10.22034/CRL.2022.329067.1154
8. Battista, F., Masala, C., Zamboni, A. *et al.* Valorisation of Agricultural Digestate for the Ammonium Sulfate Recovery and Soil Improvers Production. *Waste Biomass Valor* 12, 6903–6916 (2021). https://doi.org/10.1007/s12649-021-01486-y.
9. Branca, T. A., Colla, V., Algermissen, D., Granbom, H., Martini, U., Morillon, A., Pietruck, R., & Rosendahl, S. (2020). Reuse and recycling of by-products in the steel sector: Recent achievements paving the way to circular economy and industrial symbiosis in Europe. *Metals, 10*(3), 345. https://doi.org/10.3390/met10030345
10. Bugdayci, M., Deniz, G., Ziyreker, C., Turan, A., & Oncel, L. (2020). Thermodynamic modeling and production of FeCo alloy from mill scale through metallothermic reduction. *Engineering Science and Technology, an International Journal, 23*(5), 1259–1265. https://doi.org/10.1016/j.jestch.2020.03.003.
11. Cao, P., Long, H., Zhang, M., & Zheng, Y. (2021). Separation and recovery of iron and arsenic from acid leaching wastewater by valence state transformation. *Journal of Environmental Chemical Engineering, 9*(5), Article 105871. https://doi.org/10.1016/j.jece.2021.105871.
12. Chen, J.-A., Li, M., Deng, X., Zhang, W., Liu, Y., Huang, Z., Yang, H., & Li, X. (2024). Transforming waste to power: Selective control of associated impurity from ferrous sulfate waste for the preparation of self-doped $LiFePO_4$. *SSRN Electronic Journal*. https://doi.org/10.2139/ssrn.5039140.
13. Chernysh, Y., Yakhnenko, O., Chubur, V., & Roubík, H. (2021). Phosphogypsum recycling: A review of environmental issues, current trends, and prospects. *Applied Sciences, 11*(4), 1575. https://doi.org/10.3390/app11041575.
14. Costamagna, P., Delucchi, M., Busca, G., & Giordano, A. (2020). System for ammonia removal from anaerobic digestion and associated ammonium sulfate production: Simulation and design considerations. *Process Safety and Environmental Protection, 144*, 133–146. https://doi.org/10.1016/j.psep.2020.05.055.
15. Czaplicka, N., & Konopacka-Łyskawa, D. (2020). Utilization of gaseous carbon dioxide and industrial Ca-rich waste for calcium carbonate precipitation: A review. *Energies, 13*(23), 6239. https://doi.org/10.3390/en13236239.
16. Deng, H., Wang, H., Hao, Y., Chen, S., & Zhang, W. (2024). Reclamation of acid with electrodialysis process: Influence of selective ion-exchange membranes. *Separation and Purification Technology, 340*, Article 126774. https://doi.org/10.1016/j.seppur.2024.126774.
17. Du, M.-S., Long, B., Mei, Z.-Y., Li, Y.-S., Li, S., Wu, X.-Q., Chi, R.-A., Tan, Y.-Z., & Li, D.-S. (2025). Toward zero-waste phosphogypsum valorization: Reengineered reverse-direct flotation synchronizes gypsum purification and functional co-products production. *Chemical Engineering Journal, 517*, Article 164341. https://doi.org/10.1016/j.cej.2025.164341
18. Fan, C., Pan, F., Zhu, Q., & Wang, Z. (2025). Hydrogen direct reduction: History and pathways for cost reduction. *cScience, 5*(12), 102529. https://doi.org/10.1002/csc3.70003.
19. Furmanski, L. M., Ferreira, L. P., Nuernberg, J. B., Muller, T. G., Cargnin, M., Arnt, Â. B. C., Rocha, M. R., Zaccaron, A., Dal-Bó, A. G., & Peterson, M. (2025). Chemical synthesis of ferrous sulfate monohydrate using mill scale. *Materials Chemistry and Physics, 333*, Article 130321. https://doi.org/10.1016/j.matchemphys.2024.130321.
20. Furmanski, L. M., Müller, T. G., Nuernberg, J. B., Martins, M. A., Cargnin, M., Arnt, Â. B. C., Dal-Bó, A. G., & Peterson, M. (2024). Efficient production of ferrous sulfate from steel mill scale waste. *Journal of Sustainable Metallurgy, 10*(3), 1234–1248. https://doi.org/10.1007/s40831-024-00900-8.
21. Gan, M., Guo, E.-D., Li, H.-R., Cao, Y.-C., Fan, X.-H., Ji, Z.-Y., & Sun, Z.-Q. (2025). New technology for preparing high sphericity iron powder by hydrogen reduction: Regulation mechanism of iron particle spheroidization. *Powder Technology, 455*, Article 120254. https://doi.org/10.1016/j.powtec.2025.120254.
22. Gan, M., Guo, E.-D., Li, H.-R., Cao, Y.-C., Fan, X.-H., Ji, Z.-Y., & Sun, Z.-Q. (2024). Production of ultrafine iron powder by low-temperature hydrogen reduction: Properties change with temperature. *Journal of Iron and Steel Research International, 31*(11), 2645–2654. https://doi.org/10.1007/s42243-024-01228-z.
23. Grengs, A., Ledesma, G., Xiong, Y., Katsev, S., Poulton, S. W., Swanner, E. D., & Wittkop, C. (2024). Direct precipitation of siderite in ferruginous environments. *Geochemical Perspectives Letters, 30*, 45–50. https://doi.org/10.7185/geochemlet.2414.
24. Guo, H., Yuan, P., Pavlovic, V., Barber, J., & Kim, Y. (2021a). Ammonium sulfate production from wastewater and low-grade sulfuric acid using bipolar- and cation-exchange membranes. *Journal of Cleaner*

Production, 300, Article 124888. https://doi.org/10.1016/j.jclepro.2020.124888.

25. Guo, Z., Zhu, D.-Q., Pan, J., Yang, C., Zhang, F., Wang, Q., Li, S., & Wang, D. (2021b). Efficient and green treatment of ultrapure magnetite to prepare powder metallurgy iron powders. *Powder Technology, 378*, 19–28. https://doi.org/10.1016/j.powtec.2020.09.057.
26. Harvey, J.-P., Lebreux-Desilets, F., Marchand, J., Oishi, K., Bouarab, A.-F., Robelin, C., Gheribi, A. E., & Pelton, A. D. (2020). On the application of the FactSage thermochemical software and databases in materials science and pyrometallurgy. *Processes, 8*(9), 1156. https://doi.org/10.3390/pr8091156.
27. He, M., Shuai, J., Li, H., Li, L., Liu, Q., & Liu, W. (2025). Application of waste ferrous sulfate for recovering valuable metal elements from minerals and industrial solid waste: A waste-to-wealth strategy. *Separation and Purification Technology, 376*(Part 3), Article 134058. https://doi.org/10.1016/j.seppur.2025.134058.
28. Hessels, C. J. M., Homan, T. A. M., Deen, N. G., & Tang, Y. (2022). Reduction kinetics of combusted iron powder using hydrogen. *Powder Technology, 407*, Article 117540. https://doi.org/10.1016/j.powtec.2022.117540.
29. Hessels, C. J. M., Lelivelt, D. W. J., Stevens, N. C., Tang, Y., Deen, N. G., & Finotello, G. (2023). Minimum fluidization velocity and reduction behavior of combusted iron powder in a fluidized bed. *Fuel, 342*, Article 127710. https://doi.org/10.1016/j.fuel.2023.127710.
30. Hong, L., Bi, Q., Zhou, M., Ai, L., Cui, W., Sun, C., Fan, Z., Tong, S., & Chen, J. (2026). Preparation of high-purity iron powder by microwave-hydrogen coupling reduction of magnetite. *International Journal of Hydrogen Energy, 241*, Article 155449. https://doi.org/10.1016/j.ijhydene.2026.155449.
31. Hu, M., Zhu, D.-Q., Pan, J., & Li, S. (2025). Near-zero carbon iron powder from high-phosphorus oolitic pellets via hydrogen reduction–electromagnetic iron phase reconstruction–magnetic separation. *Powder Technology, 469*, Article 121719. https://doi.org/10.1016/j.powtec.2025.121719 .
32. Ibrahim, M. H., Batstone, D., Vaughan, J., & Steel, K. (2024). Electrochemical separation of sulfuric acid from magnesium sulfate solutions: Application for nickel laterite processing. *Separation and Purification Technology, 336*, Article 126291. https://doi.org/10.1016/j.seppur.2024.126291.
33. Idboufrade, A., Bouargane, B., Ennasraoui, B. *et al.* Phosphogypsum Two-Step Ammonia-Carbonation Resulting in Ammonium Sulfate and Calcium Carbonate Synthesis: Effect of the Molar Ratio OH^-/Ca^{2+} on the Conversion Process. *Waste Biomass Valor* 13, 1795–1806 (2022). https://doi.org/10.1007/s12649-021-01600-0.
34. Iljana, M., Heikkinen, E.-P., & Fabritius, T. (2021). Estimation of iron ore pellet softening in a blast furnace with computational thermodynamics. *Metals, 11*(10), 1515. https://doi.org/10.3390/met11101515.
35. Jiang, C. Z., & Tosca, N. J. (2020). Growth kinetics of siderite at 298.15 K and 1 bar. *Geochimica et Cosmochimica Acta, 274*, 97–117. https://doi.org/10.1016/j.gca.2020.01.047.
36. Jiang, Y., Peng, C., Zhou, K., Hu, Z., Zhang, G., Wu, Y., ... & Chen, W. (2023). Recovery of iron from titanium white waste for the preparation of LiFePO4 battery. *Journal of Cleaner Production, 415*, 137817..
37. Jung, IH., Van Ende, MA. Computational Thermodynamic Calculations: FactSage from CALPHAD Thermodynamic Database to Virtual Process Simulation. *Metall Mater Trans B* **51**, 1851–1874 (2020). https://doi.org/10.1007/s11663-020-01908-7.
38. Kądziołka-Gaweł, M., Adamczyk, Z., Łukowiec, D., Klimontko, J., Wojtyniak, M., & Nowak, J. (2025). Siderite decomposition kinetics—Influence of time, temperature, and isomorphous impurities. *Minerals, 15*(4), 428. https://doi.org/10.3390/min15040428.
39. Kądziołka-Gaweł, M., Nowak, J., Szubka, M., Klimontko, J., & Wojtyniak, M. (2023). Thermal decomposition of siderite and characterization of the decomposition products under O_2 and CO_2 atmospheres. *Minerals, 13*(8), 1066. https://doi.org/10.3390/min13081066.
40. Kaljunen, J. U., Al-Juboori, R. A., Mikola, A., Righetto, I., & Konola, I. (2021).Newly developed membrane contactor-based N and P recovery process: Pilot-scale field experiments and cost analysis. *Journal of Cleaner Production, 287*, Article 125288. https://doi.org/10.1016/j.jclepro.2020.125288.
41. Kazanç, F., Zhang, P., Saha, P., & Lu, Y. (2024). Techno-economic and life cycle environmental assessments of CO_2 utilization for value-added precipitated calcium carbonate and ammonium sulfate fertilizer co-production. *Journal of CO_2 Utilization, 84*, Article 102992. https://doi.org/10.1016/j.jcou.2024.102992.
42. Kleiber, S., Böhm, A., & Lux, S. (2024). Effect of pressure on direct reduction of mineral iron carbonate with hydrogen. *Chemical Engineering Journal, 494*, Artikel 152985. https://doi.org/10.1016/j.cej.2024.152985.
43. Koo, T.-H., & Kim, J. (2020). Controls on the formation and stability of siderite ($FeCO_3$) and chukanovite ($Fe_2(CO_3)(OH)_2$) in reducing environment. *Minerals, 10*(2), 156. https://doi.org/10.3390/min10020156.
44. Koivisto, E. S., Reuter, T., & Zevenhoven, R. (2023). Performance optimization of bipolar membrane

electrodialysis of ammonium sulfate/bisulfate reagents for CO_2 mineralization. *ACS ES&T Water, 3*(4), 1038–1049. https://doi.org/10.1021/acsestwater.3c00028.

45. Krum, K., Patil, R., Christensen, H., Hashemi, H., Glarborg, P., Marshall, P., Alzueta, M. U., & Klippenstein, S. J. (2021). Kinetic modeling of urea decomposition and byproduct formation. *Chemical Engineering Science, 230*, Article 116138. https://doi.org/10.1016/j.ces.2020.116138.
46. Kuntz, C., Kuhn, C., Weickenmeier, H., Tischer, S., Börnhorst, M., & Deutschmann, O. (2021). Kinetic modeling and simulation of high-temperature by-product formation from urea decomposition. *Chemical Engineering Science, 246*, Article 116876. https://doi.org/10.1016/j.ces.2021.116876.
47. Li, S., Zhang, H., Nie, J., Dewil, R., Baeyens, J., & Deng, Y. (2021). The direct reduction of iron ore with hydrogen. *Sustainability, 13*(16), 8866. https://doi.org/10.3390/su13168866.
48. Li, J., Zhang, T., Wang, Q., Liu, Y., Zhao, B., & Chen, X. (2022). Calcium recovery from waste carbide slag via ammonium sulfate leaching system. *Separation and Purification Technology, 291*, Article 120948. https://doi.org/10.1016/j.seppur.2022.120948
49. Loder, A., Santner, S., Siebenhofer, M., Böhm, A., & Lux, S. (2022). Reaction kinetics of direct reduction of mineral iron carbonate with hydrogen: Determination of the kinetic triplet. *Chemical Engineering Research and Design, 188*, 575–589. https://doi.org/10.1016/j.cherd.2022.10.007.
50. Ma, Y., Souza Filho, I.R., Zhang, X. *et al.* Hydrogen-based direct reduction of iron oxide at 700°C: Heterogeneity at pellet and microstructure scales. *Int J Miner Metall Mater* 29, 1901–1907 (2022). https://doi.org/10.1007/s12613-022-2440-5.
51. Maia, L. C., Santos, G. R., Gurgel, L. V. A., & Carvalho, C. F. (2020). Iron recovery from the coarse fraction of basic oxygen furnace sludge. Part I: Optimization of acid leaching conditions. *Environmental Science and Pollution Research, 27*(27), 34078–34089. https://doi.org/10.1007/s11356-020-09910-x.
52. Matei, E., Predescu, A. M., Șăulean, A. A., Râpă, M., Sohaciu, M. G., Coman, G., Berbecaru, A.-C., Predescu, C., Vâju, D., & Vlad, G. (2022). Ferrous industrial wastes—Valuable resources for water and wastewater decontamination. *International Journal of Environmental Research and Public Health, 19*(21), 13951. https://doi.org/10.3390/ijerph192113951.
53. Mend, B., Kim, J.-H. J., & Chu, Y.-S. (2026). Recovery of ferrous sulfate from basic oxygen furnace sludge using waste sulfuric acid. *MethodsX, 16*, Article 103960. https://doi.org/10.1016/j.mex.2026.103960.
54. Miškovičová, Z., Legemza, J., Demeter, P., Buľko, B., Hubatka, S., Hrubovčáková, M., Futáš, P., & Findorák, R. (2024). An overview analysis of current research status in iron oxides reduction by hydrogen. *Metals, 14*(5), 589. https://doi.org/10.3390/met14050589.
55. Moreira, V. R., Lebron, Y. A. R., Gontijo, D., & Amaral, M. C. S. (2022). Membrane distillation and dispersive solvent extraction in a closed-loop process for water, sulfuric acid and copper recycling from gold mining wastewater. *Chemical Engineering Journal, 435*, Article 133874. https://doi.org/10.1016/j.cej.2021.133874.
56. Moreira, V. R., Lebron, Y. A. R., Gontijo, D., & Amaral, M. C. S. (2022b). One-step recycling of mineral acid from concentrated gold mining wastewater by high-temperature liquid–liquid extraction. *Separation and Purification Technology, 286*, Article 120447. https://doi.org/10.1016/j.seppur.2022.120447.
57. Mulders, J. J. P. A., Tobler, D. J., & Oelkers, E. H. (2021). Siderite nucleation pathways as a function of aqueous solution saturation state at 25 °C. *Chemical Geology, 559*, Article 119947. https://doi.org/10.1016/j.chemgeo.2020.119947.
58. Neerup, R., Løge, I. A., & Fosbøl, P. L. (2023). $FeCO_3$ synthesis pathways: The influence of temperature, duration, and pressure. *ACS Omega, 8*(3), 3404–3414. https://doi.org/10.1021/acsomega.2c07303.
59. Orabi, A. S., Ismail, A. H., Abou El-Nour, K. M., Atia, B. M., Gado, M. A., Cheira, M. F., & Goda, A. E.-S. (2024). The employing of pure calcium sulfate extracted from phosphogypsum for composing highly pure ammonium sulfate and calcium carbonate. *Canadian Metallurgical Quarterly, 63*(4), 1554–1571. https://doi.org/10.1080/00084433.2024.2305998.
60. Page, M. J., McKenzie, J. E., Bossuyt, P. M., Boutron, I., Hoffmann, T. C., Mulrow, C. D., Shamseer, L., Tetzlaff, J. M., Akl, E. A., Brennan, S. E., Chou, R., Glanville, J., Grimshaw, J. M., Hróbjartsson, A., Lalu, M. M., Li, T., Loder, E. W., Mayo-Wilson, E., McDonald, S., … Moher, D. (2021). The PRISMA 2020 statement: An updated guideline for reporting systematic reviews. *BMJ, 372*, n71. https://doi.org/10.1136/bmj.n71.
61. Pang, H., Lu, R., Zhang, T., Lü, L., Chen, Y., & Tang, S. (2020). Chemical dehydration coupling multi-effect evaporation to treat waste sulfuric acid in titanium dioxide production process. *Chinese Journal of Chemical Engineering, 28*(4), 1162–1170. https://doi.org/10.1016/j.cjche.2020.02.009.
62. Pickles, C. A., & Marzoughi, O. (2022). Thermodynamic modelling of decomposition processes in the Mn–O and Mn–O–H systems. *Canadian Metallurgical Quarterly, 62*(4), 1–20. https://doi.org/10.1080/00084433.2022.2060602.
63. Qiu, Z., Zhou, K., Peng, C., Lei, Q., Jiang, Y., Zhou, H., & Chen, W. (2025). Preparation of battery-grade

iron phosphate from iron-rich waste acid in titanium white production. *Journal of Cleaner Production, 524*, Article 146492. https://doi.org/10.1016/j.jclepro.2025.146492.

64. Ren, G. (2025). Microwave-assisted reduction technology for recycling of hematite nanoparticles from ferrous sulfate residue. *Materials, 18*(14), 3214. https://doi.org/10.3390/ma18143214.
65. Rongwong, W., Bae, T.-H., & Jiraratananon, R. (2022). Economic optimization of hollow fiber membrane contactors for ammonia nitrogen recovery from anaerobic digestion effluents. *Journal of Environmental Chemical Engineering, 10*(3), Article 108631. https://doi.org/10.1016/j.jece.2022.108631.
66. Shao, H., Zhang, Y., Liu, X., Wang, Z., Li, J., & Chen, Y. (2025). Preparation of battery-grade Fe_2O_3 and $FePO_4{\cdot}2H_2O$ materials from ferrous sulfate waste by chemical precipitation. *Journal of Environmental Chemical Engineering, 13*(4), Article 115127. https://doi.org/10.1016/j.jece.2025.115127.
67. Souza Filho, I. R., Springer, H., Ma, Y., Mahajan, A., da Silva, C. C., Kulse, M., & Raabe, D. (2022). *Green steel at its crossroads: Hybrid hydrogen-based reduction of iron ores*. *Journal of Cleaner Production, 340*, Article 130805. https://doi.org/10.1016/j.jclepro.2022.130805.
68. Srivastava, S., Jacklin, R., Snellings, R., Meynen, V., Elsen, J., & Cool, P. (2022). Experiments and modelling to understand $FeCO_3$ cement formation mechanism: Time-evolution of CO_2-species, dissolved-Fe, and pH during CO_2-induced dissolution of Fe(0). *Construction and Building Materials, 345*, Article 128281. https://doi.org/10.1016/j.conbuildmat.2022.128281.
69. Srivastava, S., Snellings, R., Meynen, V., & Cool, P. (2020). Utilising the principles of $FeCO_3$ scaling for cementation in H_2O–CO_2(g)–Fe system. *Corrosion Science, 169*, Article 108613. https://doi.org/10.1016/j.corsci.2020.108613.
70. Swain, B., Akcil, A., & Lee, J.-C. (2022). Red mud valorization: An industrial waste circular economy challenge; Review over processes and their chemistry. *Critical Reviews in Environmental Science and Technology, 52*(4), 520–570. https://doi.org/10.1080/10643389.2020.1829898.
71. Tang, Z., Xiao, H., Sun, Y., Gao, P., & Zhang, Y. (2022). Exploration of hydrogen-based suspension magnetization roasting for refractory iron ore towards a carbon-neutral future: A pilot-scale study. *International Journal of Hydrogen Energy, 47*(33), 15074–15083. https://doi.org/10.1016/j.ijhydene.2022.02.219.
72. Vilaça, A. S. I., Simão, L., Montedo, O. R. K., Novaes de Oliveira, A. P., & Raupp-Pereira, F. (2022). Waste valorization of iron ore tailings in Brazil: Assessment metrics from a circular economy perspective. *Resources Policy, 75*, Article 102477. https://doi.org/10.1016/j.resourpol.2021.102477.
73. Wang, H., Zhang, Y., Liu, Z., Chen, X., Li, J., & Zhao, Y. (2026). Toward large-scale utilization approaches for phosphogypsum: Reclamation, purification, and stabilization strategies. *iScience, 29*, Article 115713. https://doi.org/10.1016/j.isci.2026.115713.
74. Wang, T., Qu, H., Ravindra, A. V., Ma, S., Hu, J., Zhang, H., Le, T., & Zhang, L. (2023). Treatment of complex sulfur-containing solutions in ammonia desulfurization ammonium sulfate production by ultrasonic-assisted ozone technology. *Ultrasonics Sonochemistry, 95*, Article 106386. https://doi.org/10.1016/j.ultsonch.2023.106386.
75. Wendel, J., Manchili, S. K., Hryha, E., & Nyborg, L. (2020a). Oxide reduction and oxygen removal in water-atomized iron powder: A kinetic study. *Journal of Thermal Analysis and Calorimetry, 142*(1), 309–320. https://doi.org/10.1007/s10973-020-09724-6.
76. Wendel, J., Manchili, S. K., Hryha, E., & Nyborg, L. (2020b). Reduction of surface oxide layers on water-atomized iron and steel powder in hydrogen: Effect of alloying elements and initial powder state. *Thermochimica Acta, 692*, Article 178731. https://doi.org/10.1016/j.tca.2020.178731.
77. Wu, J., Xu, B., Zhou, Y., Dong, Z., Zhong, S., & Jiang, T. (2023). A novel process of reverse flotation-hydrogen reduction for preparation of high-purity iron powder with superior magnetite concentrate. *Separation and Purification Technology, 307*, Article 122784. https://doi.org/10.1016/j.seppur.2022.122784
78. Wu, P., Zhao, L., Wang, Y., Ge, J., Li, Z., Li, Z., & Qiu, G. (2024). Preparation of lithium iron phosphate with superior electrochemical performances from titanium white by-product ferrous sulfate. *Solid State Ionics, 410*, Article 116715. https://doi.org/10.1016/j.ssi.2024.116715.
79. Xing, Y., Liu, H., Deng, Z., Wei, C., Li, X., Li, M., & Yang, Y. (2021). Dissolution behavior of ferrous sulfate in the hematite process. *Hydrometallurgy, 200*, Article 105561. https://doi.org/10.1016/j.hydromet.2021.105561.
80. Yao, G., Li, Y., Guo, Q., Qi, T., & Guo, Z. (2021). Preparation of reduced iron powder for powder metallurgy from magnetite concentrate by direct reduction and wet magnetic separation. *Powder Technology, 392*, 344–355. https://doi.org/10.1016/j.powtec.2021.07.023.
81. Yahya, M. N., Gökçekuş, H., Orhon, D., Keskinler, B., Karagunduz, A., & Omwene, P. I. (2021). A study on the hydrolysis of urea contained in wastewater and continuous recovery of ammonia by an enzymatic membrane reactor. *Processes, 9*(10), 1703. https://doi.org/10.3390/pr9101703.

82. Yuzer, B., Aydin, M. I., Yildiz, H., Hasançebi, B., Selcuk, H., et al. (2022). Optimal performance of electrodialysis process for the recovery of acid wastes in wastewater: Practicing circular economy in aluminum finishing industry. *Chemical Engineering Journal*, *434*, Article 134755. https://doi.org/10.1016/j.cej.2022.134755.
83. Zhang, C., Zhang, W., & Wang, Y. (2020). Diffusion dialysis for acid recovery from acidic waste solutions: Anion exchange membranes and technology integration. *Membranes*, *10*(8), 169. https://doi.org/10.3390/membranes10080169.
84. Zhang, H., Liu, X., Fu, L., Jia, X., & Xu, G. (2024). Updating mechanism of siderite roasting through insights into reactions between inherent oxides of iron and carbon. *Powder Technology*.
85. Zhang, Q., Sun, Y., Han, Y., Gao, P., & Li, Y. (2021). Thermal decomposition kinetics of siderite ore during magnetization roasting. *Mining, Metallurgy & Exploration*, *38*(5), 2321–2332. https://doi.org/10.1007/s42461-021-00453-5.
86. Zhang, Q., Sun, Y., Qin, Y., Gao, P., & Yuan, S. (2022). Siderite pyrolysis in suspension roasting: An in-situ study on kinetics, phase transformation, and product properties. *Journal of Central South University*, *29*(6), 1749–1760. https://doi.org/10.1007/s11771-022-5059-9.
87. Zhang, X., Liu, P., Gao, P., Li, W., Han, Y., & Li, Y. (2024). *A clean and green technology for iron extraction from refractory siderite ore via fluidization self-magnetization roasting*. *Powder Technology*, *444*, Article 119993. https://doi.org/10.1016/j.powtec.2024.119993.
88. Zhou, T., Sun, Y., Han, Y., & Li, Y. (2025). Hydrogen-based fluidization direct reduction of high purity iron concentrate: Experimental optimization and mechanism analysis. *Minerals Engineering*, *227*, Article 109273. https://doi.org/10.1016/j.mineng.2025.109273.
89. Zhou, T., Sun, Y., Han, Y., & Li, Y. (2026). Hydrogen-based direct reduction reaction behavior and isothermal kinetics of siderite. *International Journal of Hydrogen Energy, 216*, Article 153930. https://doi.org/10.1016/j.ijhydene.2026.153930.
90. Zhu, X., Han, Y., Sun, Y., Gao, P., & Li, Y. (2023). Thermal decomposition of siderite ore in different flowing atmospheres: Phase transformation and magnetism. *Mineral Processing and Extractive Metallurgy Review*, *44*(3), 201–208. https://doi.org/10.1080/08827508.2022.2040498.